



U.S. DEPARTMENT OF
ENERGY

Office of
Science

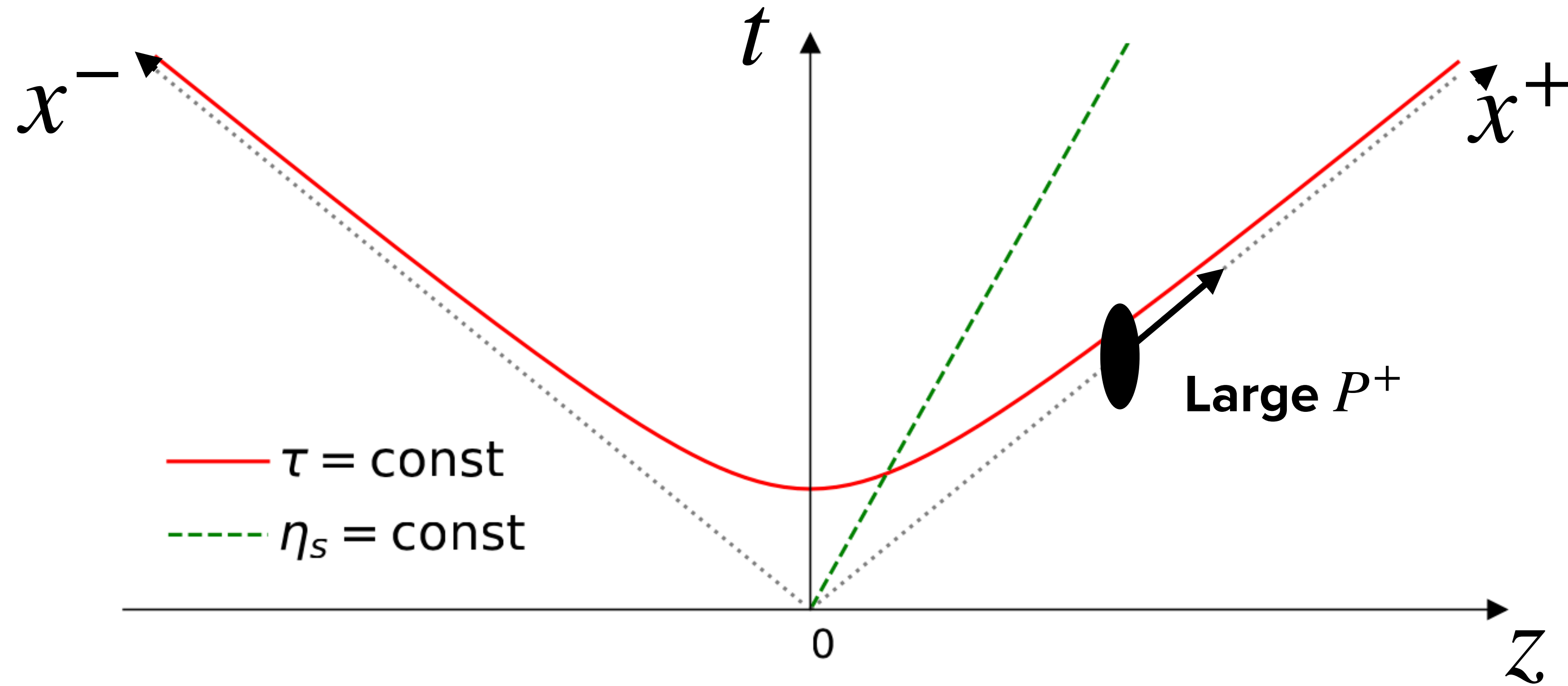
PROBING THE INITIAL STATE WITH VECTOR MESON PRODUCTION AND EXCLUSIVE DIJETS

BJÖRN SCHENKE, BROOKHAVEN NATIONAL LABORATORY

EICUG 2nd Detector Meeting
CFNS, Stony Brook University

12/6/2022

The scenario: Hadron moving at high momentum



Probe hadron (or nucleus) moving with large P^+ at scale $x_0 P^+$ with $x_0 \ll 1$

Separate partonic content based on longitudinal momentum $k^+ = xP^+$

Large $x > x_0$: Static and localized color sources ρ

Dynamic color fields

The moving color sources generate a current, independent of light cone time z^+ :

$$J^{\mu,a}(z) = \delta^{\mu+} \rho^a(z^-, z_T) \quad a \text{ is the color index of the gluon}$$

This current generates delocalized dynamical fields $A^{\mu,a}(z)$ described by the Yang-Mills equations

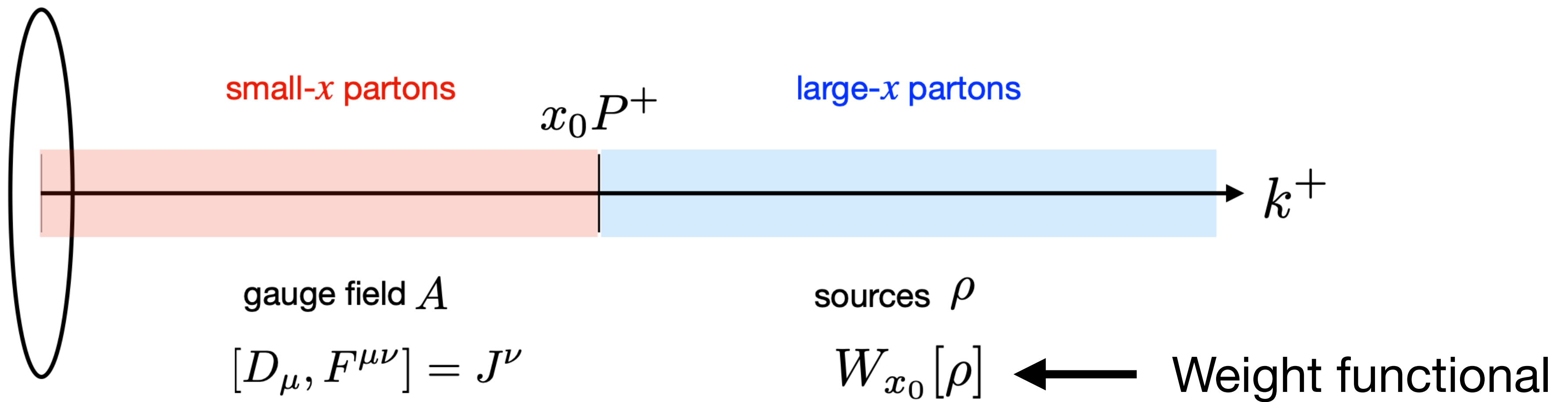
$$[D_\mu, F^{\mu\nu}] = J^\nu$$

with $D_\mu = \partial_\mu + igA_\mu$ and $F_{\mu\nu} = \frac{1}{ig}[D_\mu, D_\nu] = \partial_\mu A_\nu - \partial_\nu A_\mu + ig[A_\mu, A_\nu]$

These fields are the small $x < x_0$ degrees of freedom

They can be treated classically, because their occupation number is large $\langle AA \rangle \sim 1/\alpha_s$

Color Glass Condensate (CGC): Sources and fields



Two steps to compute expectation value of an observable \mathcal{O} :

- 1) Compute quantum expectation value $\mathcal{O}[\rho] = \langle \mathcal{O} \rangle_\rho$ for sources drawn from a given $W_{x_0}[\rho]$
- 2) Average over all possible configurations given the appropriate gauge invariant weight functional $W_{x_0}[\rho]$ (e.g. from McLerran Venugopalan model)

When $x \lesssim x_0$ the path integral $\langle \mathcal{O} \rangle_\rho$ is dominated by classical solution and we are done

For smaller x we need to do quantum evolution

Wilson lines

Interaction of high energy color-charged probe with large k^- momentum (and small $k^+ = \frac{k_T^2}{2k^-}$)

with a classical field of a nucleus can be described in the **eikonal approximation**:

The scattering rotates the color, but keeps k^- , transverse position \vec{x}_T , and any other quantum numbers the same.

The color rotation is encoded in a light-like Wilson line, which for a quark probe reads

$$V_{ij}(\vec{x}_T) = \mathcal{P} \left(ig \int_{-\infty}^{\infty} A^{+,c}(z^-, \vec{x}_T) t_{ij}^c dz^- \right)$$
$$= \sum_{n=0}^{\infty} (gA_{\text{cl}}^+)^n$$

MULTIPLE
INTERACTIONS
NEED TO BE
RESUMMED,
BECAUSE
 $A^+ \sim 1/g$

Connection between the initial state of heavy ion collisions ands the EIC

- These Wilson lines are the building blocks of the CGC
- In heavy ion collisions, one can compute the initial state by determining Wilson lines after the collision from the Wilson lines of the colliding nuclei
- At the EIC (and HERA and in UPCs), cross sections will be calculated as convolutions of Wilson line correlators with perturbatively calculable and process-dependent impact factors
- This allows the computation of rather direct constraints for the initial state of heavy ion collisions from electron-nucleus (γ -nucleus) or electron-proton collisions
- Here: Diffractive vector meson and dijet production, and DVCS (see Farid's talk on Thursday for inclusive dijets)

Heavy ion collision

Compute gluon fields after the collision using light cone gauge:

$A^+ = 0$ for a right moving nucleus, $A^- = 0$ for a left moving nucleus

gauge transformation: $A_\mu(x) \rightarrow V(x) \left(A_\mu(x) - \frac{i}{g} \partial_\mu \right) V^\dagger(x)$

using our Wilson lines $V^\dagger(x^-, \mathbf{x}_\perp) = \mathcal{P} \exp \left(-ig \int_{-\infty}^{x^-} dz^- A^+(z^-, \mathbf{x}_\perp) \right)$ (for the right moving nucleus)

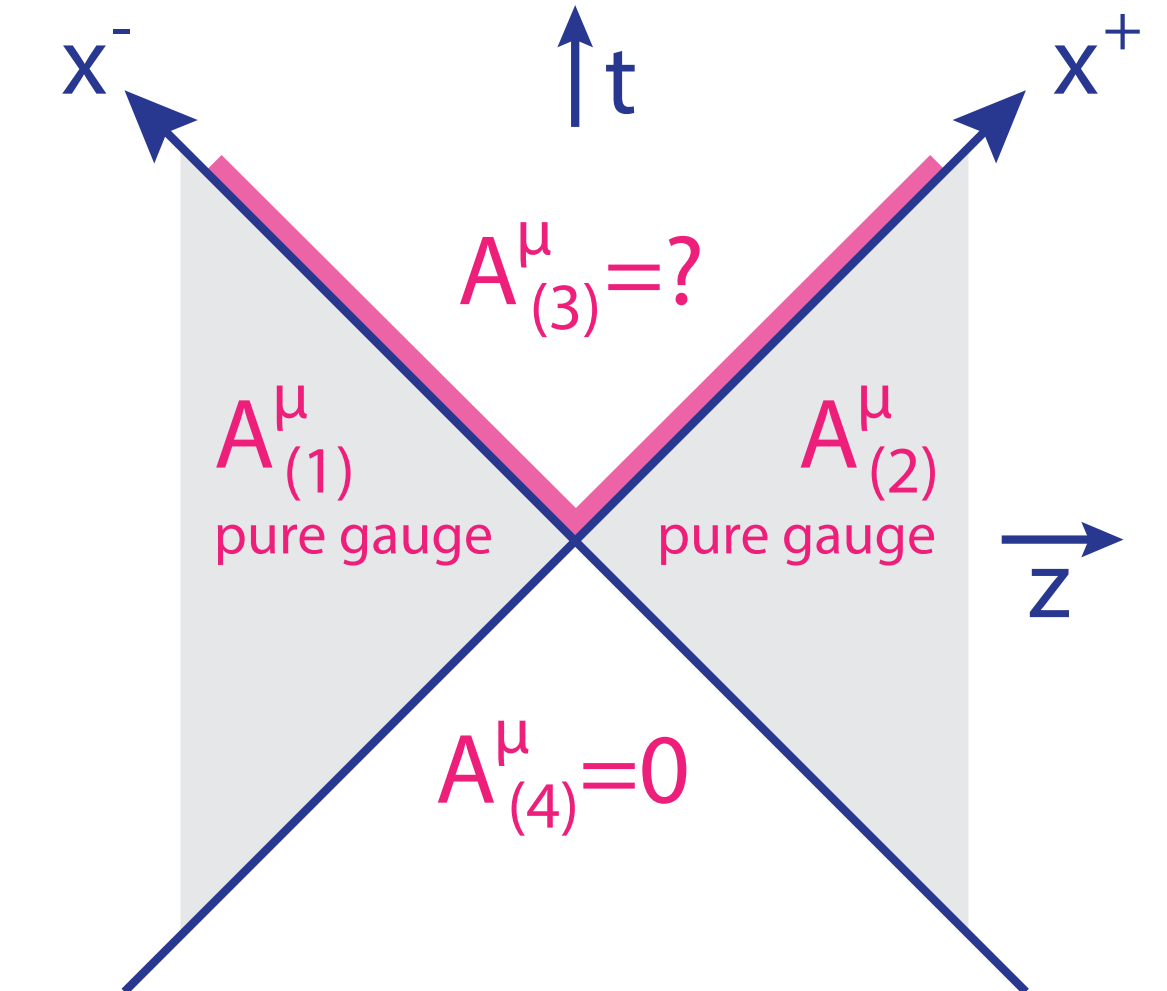
Then, the gauge fields read (choosing $A^\mu = 0$ for the quadrant for $x^- < 0$ and $x^+ < 0$)

$$A^i(x) = \theta(x^+) \theta(x^-) \alpha_P^i(\tau, \mathbf{x}_\perp) + \theta(x^-) \theta(-x^+) \alpha_T^i(\mathbf{x}_\perp) + \theta(x^+) \theta(-x^-) \alpha_P^i(\mathbf{x}_\perp)$$

$$A^\eta(x) = \theta(x^+) \theta(x^-) \alpha^\eta(\tau, \mathbf{x}_\perp)$$

with $\alpha_P^i(\mathbf{x}_\perp) = \frac{1}{ig} V_P(\mathbf{x}_\perp) \partial^i V_P^\dagger(\mathbf{x}_\perp)$ and $\alpha_T^i(\mathbf{x}_\perp) = \frac{1}{ig} V_T(\mathbf{x}_\perp) \partial^i V_T^\dagger(\mathbf{x}_\perp)$

$A^\tau = 0$, because we chose Fock-Schwinger gauge $x^+ A^- + x^- A^+ = 0$



Heavy ion collision

Plugging this ansatz

$$A^i(x) = \theta(x^+) \theta(x^-) \alpha^i(\tau, \mathbf{x}_\perp) + \theta(x^-) \theta(-x^+) \alpha_P^i(\mathbf{x}_\perp) + \theta(x^+) \theta(-x^-) \alpha_T^i(\mathbf{x}_\perp)$$
$$A^\eta(x) = \theta(x^+) \theta(x^-) \alpha^\eta(\tau, \mathbf{x}_\perp)$$

into YM equations leads to singular terms on the boundary from derivatives of θ -functions

Requiring that the singularities vanish leads to the solutions

$$\alpha^i = \alpha_P^i + \alpha_T^i \quad \alpha^\eta = -\frac{ig}{2} [\alpha_{Pj}, \alpha_T^j] \quad \partial_\tau \alpha^i = 0$$
$$\partial_\tau \alpha^\eta = 0$$

These are the gauge fields in the forward light cone.

We can compute $T^{\mu\nu}$ from it, providing an initial condition for hydrodynamics.

Geometry, fluctuations, ...

- All the information on geometry and nucleon and sub-nucleon fluctuations is contained in the distribution of color charges $\rho_{P/T}^a(x^\mp, \mathbf{x}_\perp)$
- Typically, use the MV model, which gives
$$\langle \rho^a(\mathbf{b}_\perp) \rho^b(\mathbf{x}_\perp) \rangle = g^2 \mu^2(x, \mathbf{b}_\perp) \delta^{ab} \delta^{(2)}(\mathbf{b}_\perp - \mathbf{x}_\perp)$$
- The color charge distribution $g^2 \mu(x, \mathbf{b}_\perp)$ depends on the longitudinal momentum fraction x and the transverse position \mathbf{b}_\perp . The latter needs to be modeled, the former can be modeled or obtained from e.g. JIMWLK evolution
- We factorize $\mu(x, \mathbf{b}_\perp) \sim T(\mathbf{b}_\perp) \mu(x)$ and constrain the impact parameter \mathbf{b}_\perp dependence using input from a process sensitive to geometry, such as diffractive VM production
- The cross section for that process can be expressed with the Wilson lines of the target
The same quantities we have used to initialize the heavy ion collision

Diffractive vector meson production

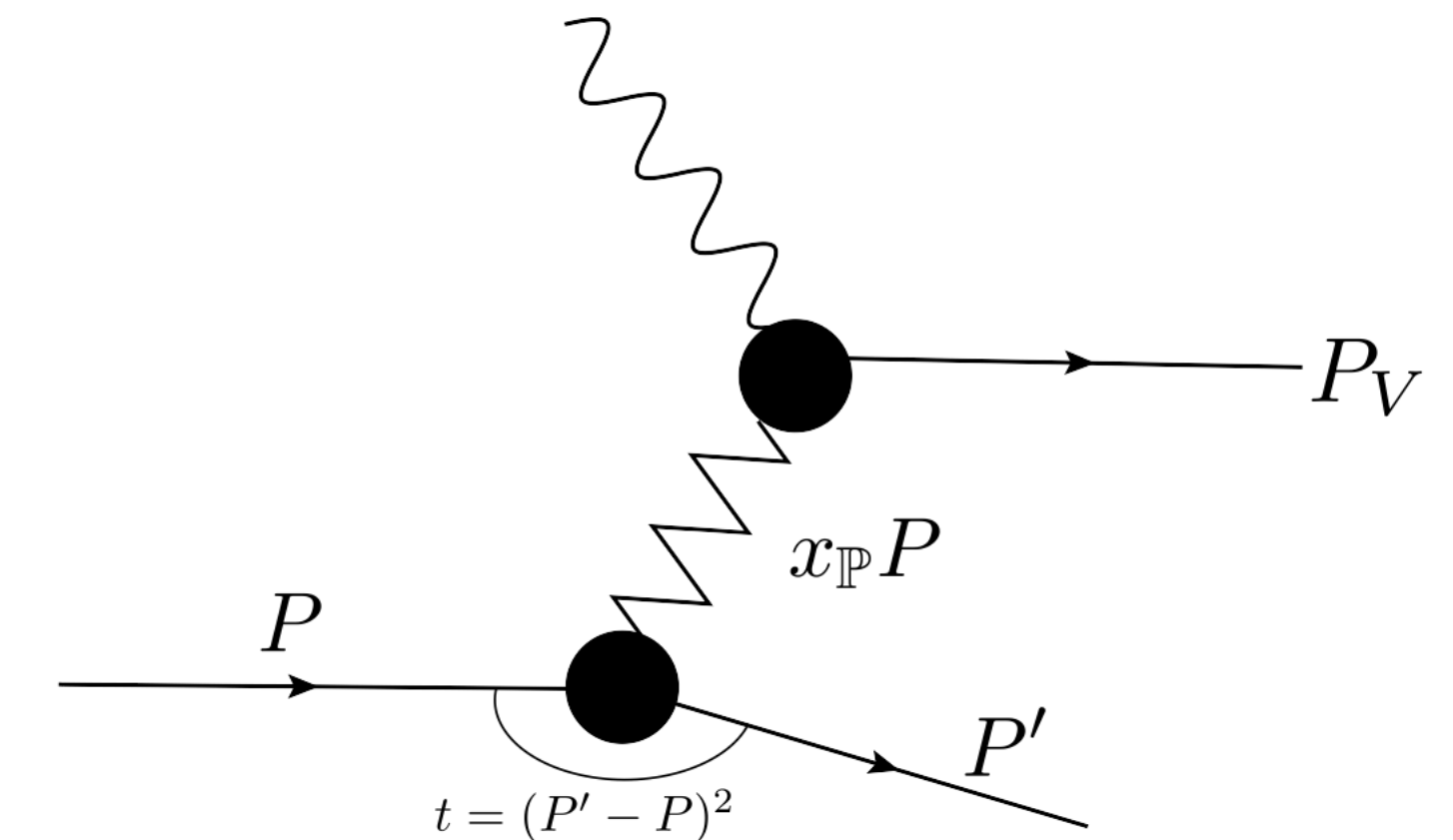
- Coherent diffraction: $\frac{d\sigma^{\gamma^* p \rightarrow Vp}}{dt} = \frac{1}{16\pi} \left| \left\langle A^{\gamma^* p \rightarrow Vp} (x_P, Q^2, \vec{\Delta}) \right\rangle \right|^2$
Target stays intact
- Incoherent diffraction: $\frac{d\sigma^{\gamma^* p \rightarrow Vp^*}}{dt} = \frac{1}{16\pi} \left(\left\langle \left| A^{\gamma^* p \rightarrow Vp} (x_P, Q^2, \vec{\Delta}) \right|^2 \right\rangle - \left| \left\langle A^{\gamma^* p \rightarrow Vp} (x_P, Q^2, \vec{\Delta}) \right\rangle \right|^2 \right)$
Target breaks up

M. L. Good and W. D. Walker, Phys. Rev. 120 (1960) 1857

H. I. Miettinen and J. Pumplin, Phys. Rev. D18 (1978) 1696

Y. V. Kovchegov and L. D. McLerran, Phys. Rev. D60 (1999) 054025

A. Kovner and U. A. Wiedemann, Phys. Rev. D64 (2001) 114002

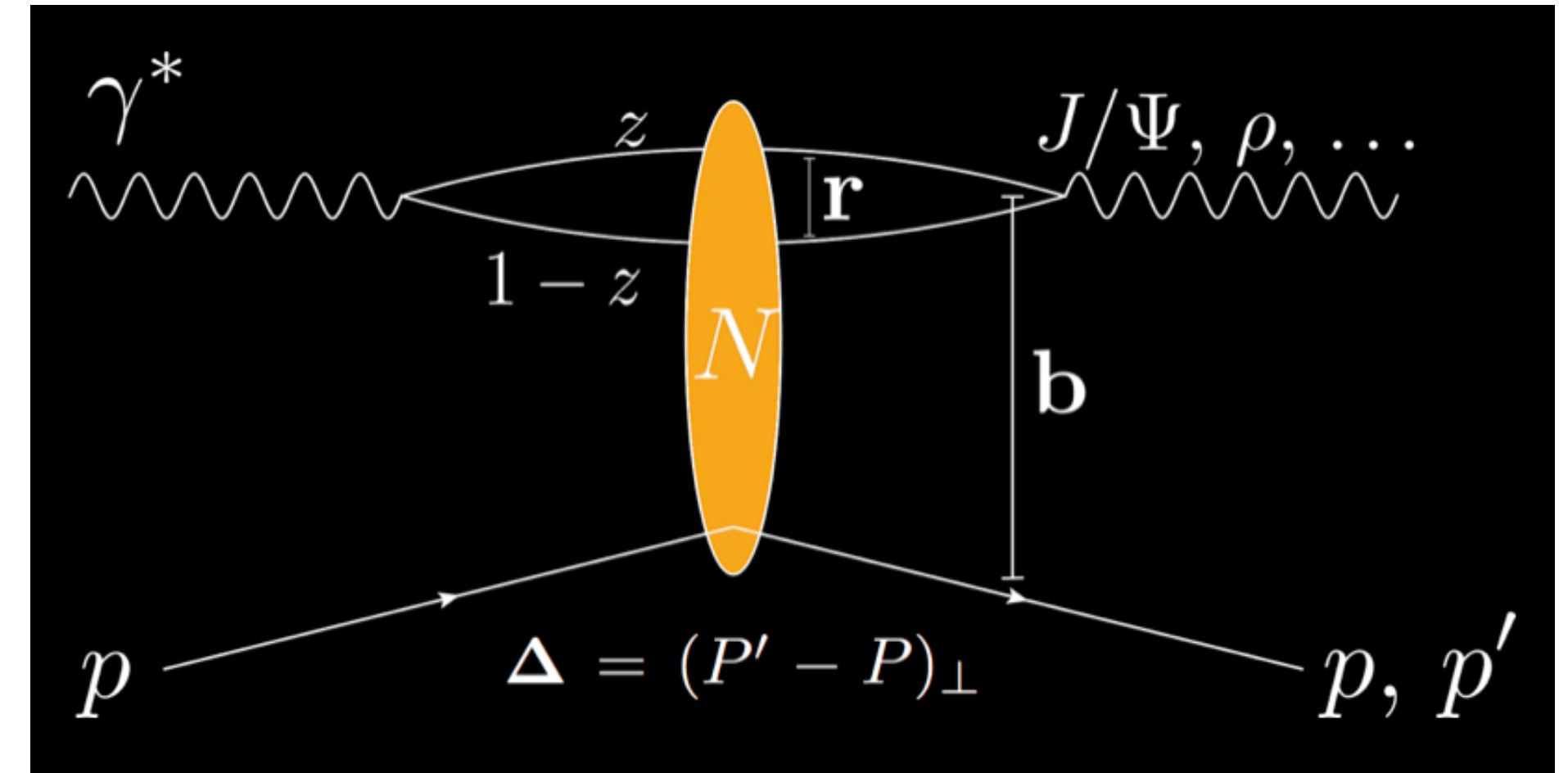


Dipole picture: Scattering amplitude

H. Mäntysaari, B. Schenke, Phys. Rev. Lett. 117 (2016) 052301; Phys. Rev. D94 (2016) 034042

High energy factorization:

- $\gamma^* \rightarrow q\bar{q} : \psi^\gamma(r, Q^2, z)$
- $q\bar{q}$ dipole scatters with amplitude N
- $q\bar{q} \rightarrow V : \psi^V(r, Q^2, z)$



$$A \sim \int d^2b dz d^2r \psi^*(\vec{r}, z, Q^2) \psi^V(\vec{r}, z, Q^2) e^{-i\vec{b} \cdot \vec{\Delta}} N(\vec{r}, x, \vec{b})$$

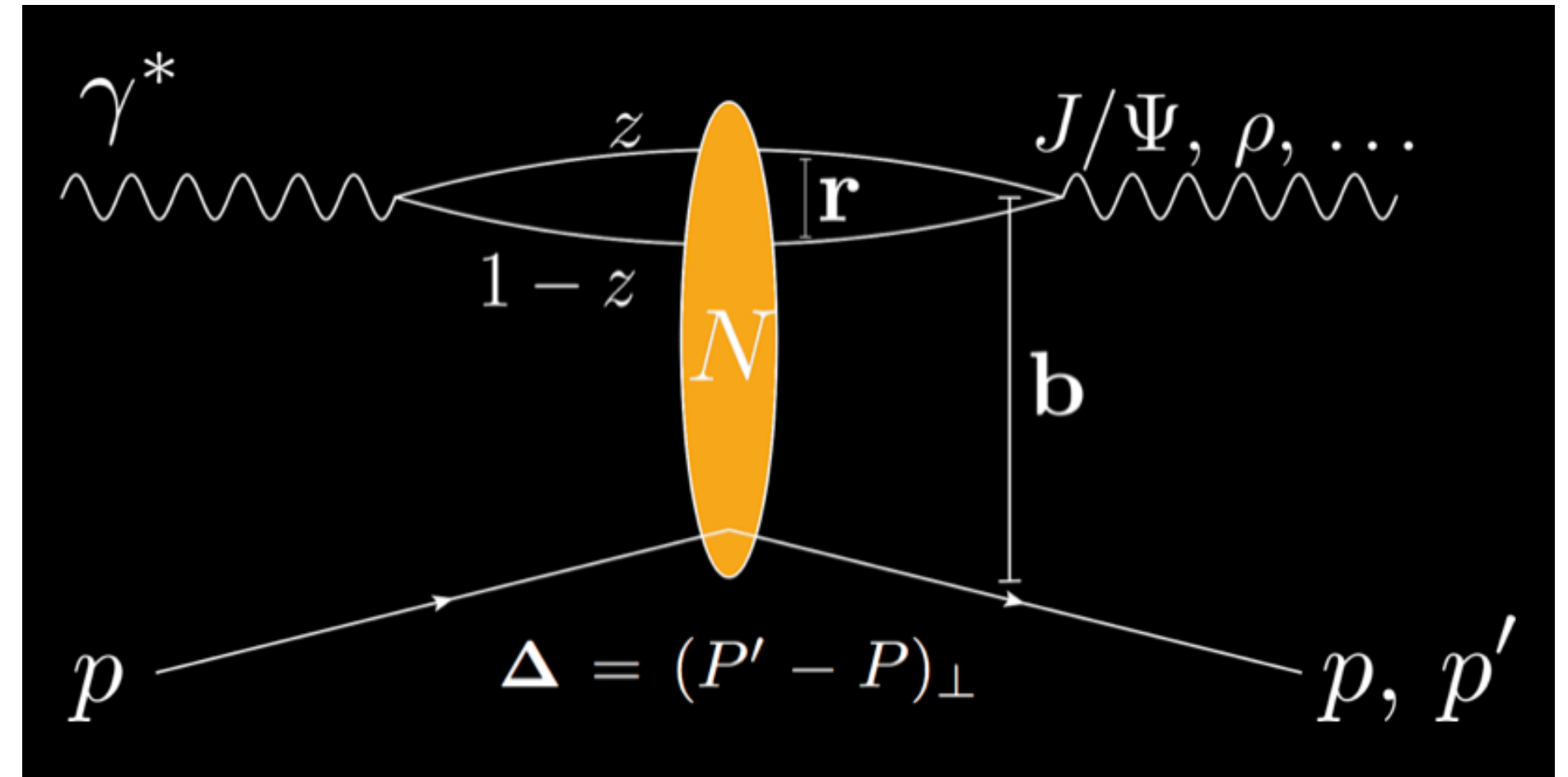
- Impact parameter \mathbf{b} is the Fourier conjugate of transverse momentum transfer $\mathbf{\Delta} \rightarrow$ Access spatial structure ($t = -\Delta^2$)
- Total F_2 : forward scattering amplitude ($\mathbf{\Delta}=0$) for $V=\gamma$ (same N)

Color glass condensate formalism

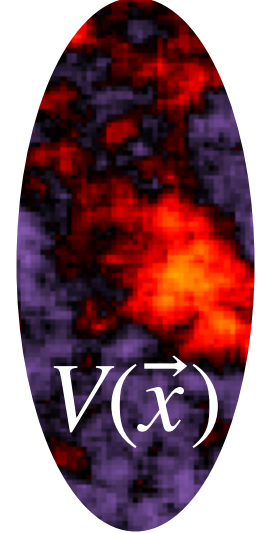
H. Mäntysaari, B. Schenke, Phys.Rev.D 98 (2018) 3, 034013

Compute the Wilson lines as before using color charges whose correlator depends on \vec{b}_\perp

$$\langle \rho^a(\mathbf{b}_\perp) \rho^b(\mathbf{x}_\perp) \rangle = g^2 \mu^2(x, \mathbf{b}_\perp) \delta^{ab} \delta^{(2)}(\mathbf{b}_\perp - \mathbf{x}_\perp)$$



$$N(\vec{r}, x, \vec{b}) = N(\vec{x} - \vec{y}, x, (\vec{x} + \vec{y})/2) = \text{Tr}(\mathbf{V}(\vec{x}) \mathbf{V}^\dagger(\vec{y})) / N_c$$



Evolution is done using the Langevin formulation of the JIMWLK equations

K. Rummukainen and H. Weigert Nucl. Phys. A739 (2004) 183; T. Lappi, H. Mäntysaari, Eur. Phys. J. C73 (2013) 2307

Long distance tails are tamed by imposing a regulator in the JIMWLK kernel, m

S. Schlichting, B. Schenke, Phys.Lett. B739 (2014) 313-319

Model impact parameter dependence

H. Mäntysaari, B. Schenke, Phys. Rev. Lett. 117 (2016) 052301; Phys. Rev. D94 (2016) 034042

1) Assume Gaussian proton shape:

$$T(\vec{b}) = T_p(\vec{b}) = \frac{1}{2\pi B_p} e^{-b^2/(2B_p)}$$

2) Assume Gaussian distributed and Gaussian shaped hot spots:

$$P(b_i) = \frac{1}{2\pi B_{qc}} e^{-b_i^2/(2B_{qc})} \quad (\text{angles uniformly distributed})$$

$$T_p(\vec{b}) = \frac{1}{N_q} \sum_{i=1}^{N_q} T_q(\vec{b} - \vec{b}_i) \quad \text{with } N_q \text{ hot spots;}$$

$$T_q(\vec{b}) = \frac{1}{2\pi B_q} e^{-b^2/(2B_q)}$$

Diffractive J/ψ production in e+p at HERA

Nucleon parameters B_q , B_{qc} , can be constrained by e+p scattering data from HERA

Exclusive diffractive J/Ψ production in e+p:

Incoherent x-sec sensitive to fluctuations

H. Mäntysaari, B. Schenke, Phys. Rev. Lett. 117 (2016) 052301

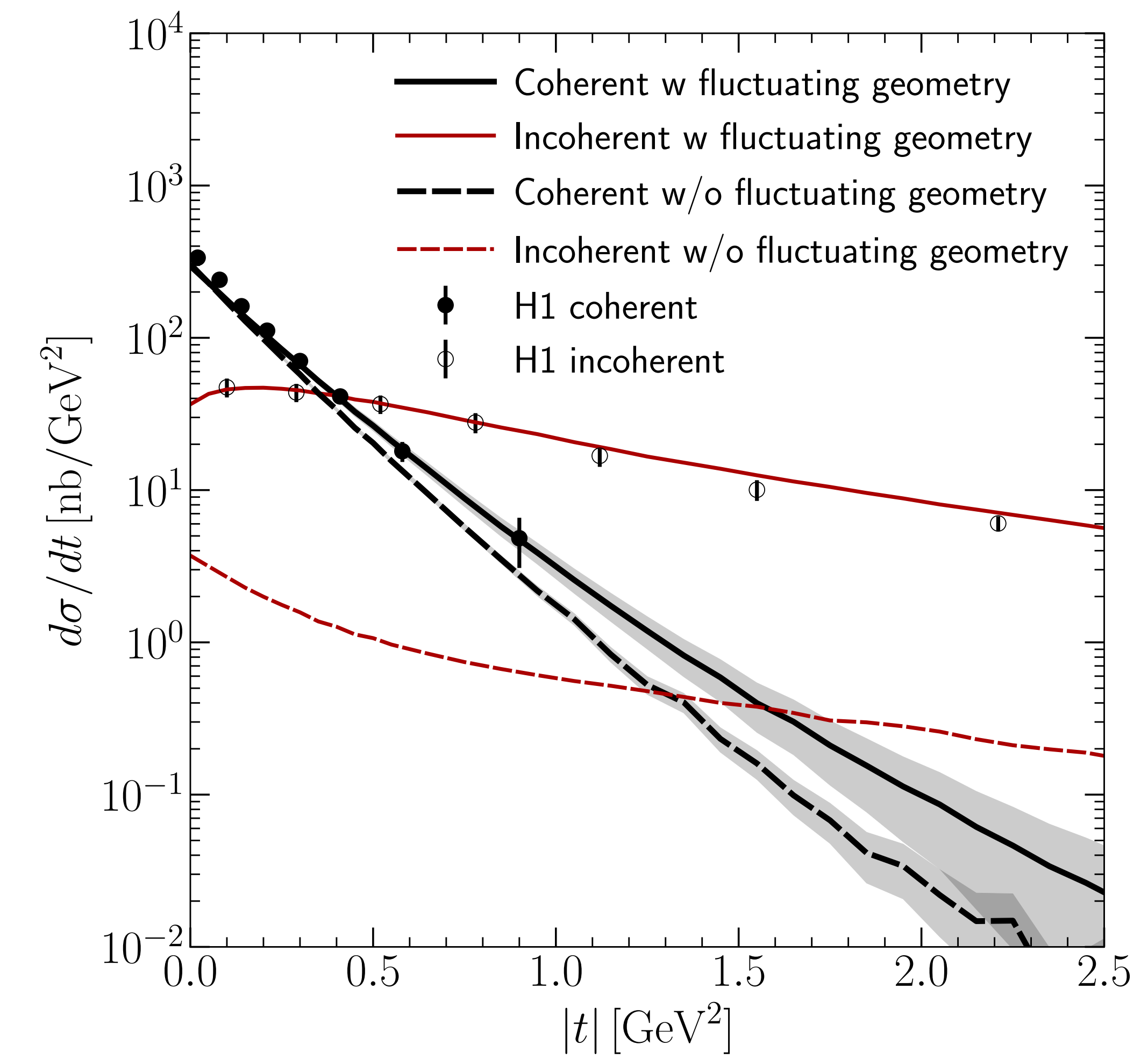
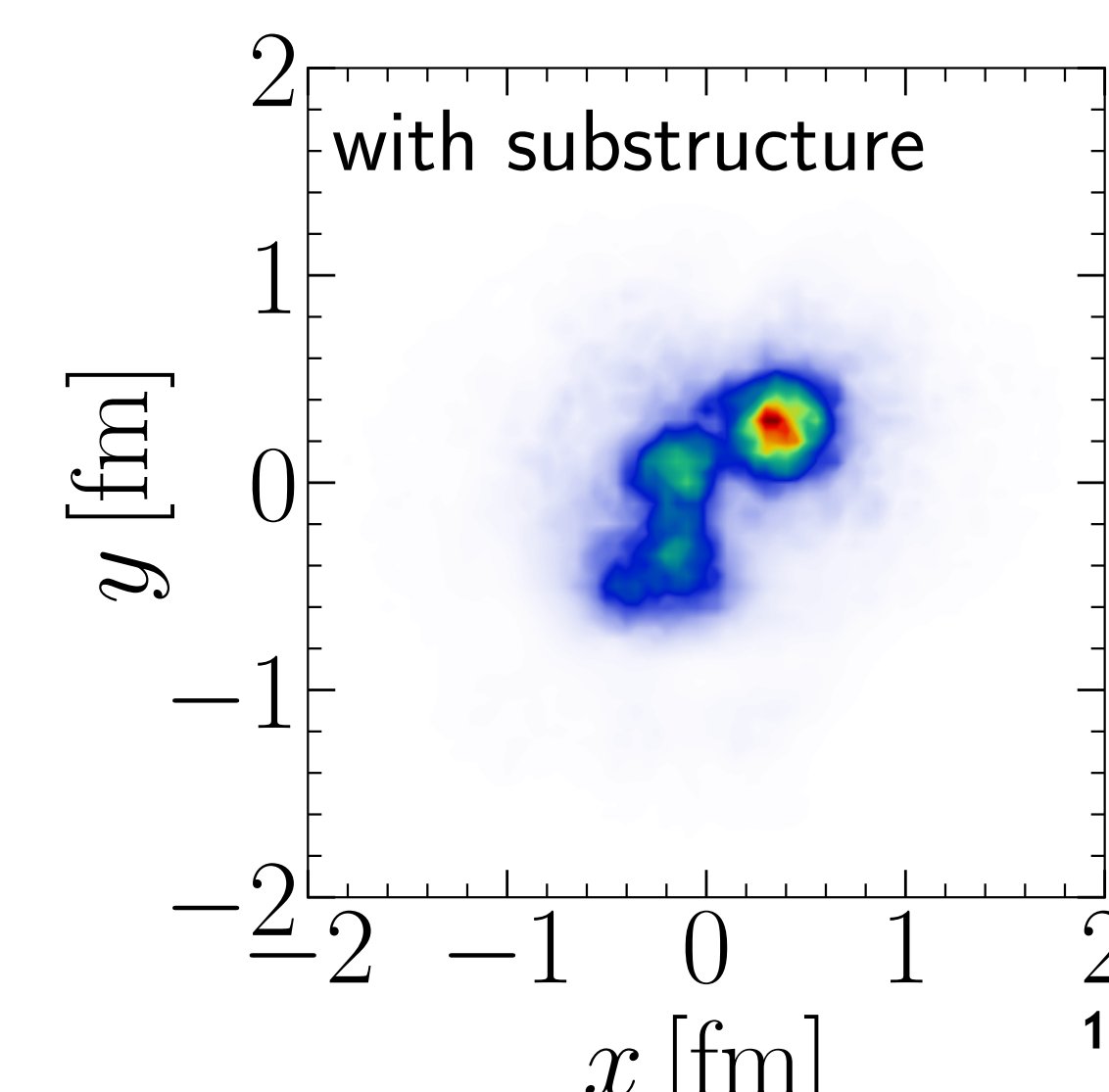
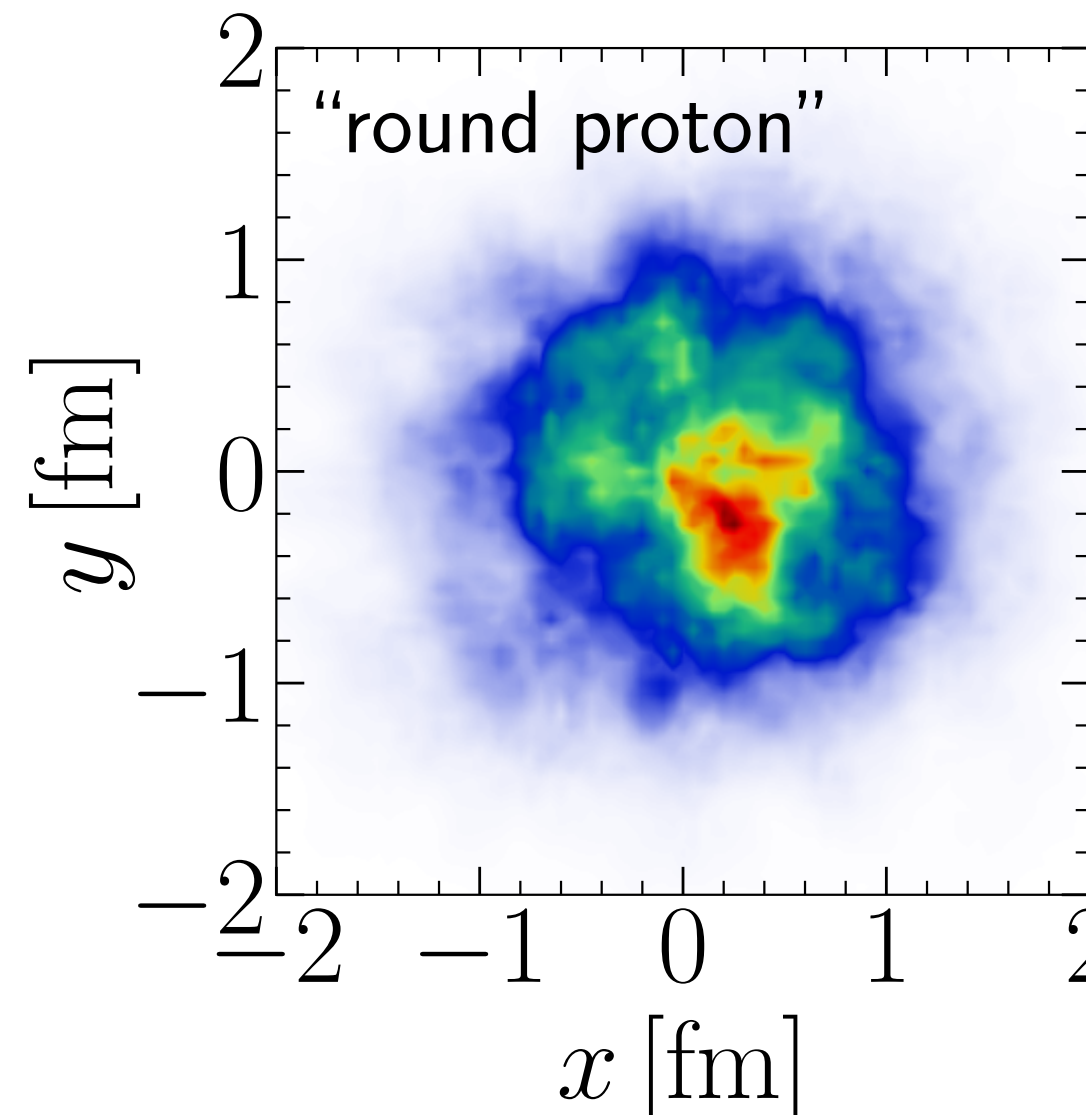
Phys. Rev. D94 (2016) 034042

also see:

S. Schlichting, B. Schenke, Phys. Lett. B739 (2014) 313-319

H. Mäntysaari, Rep. Prog. Phys. 83 082201 (2020)

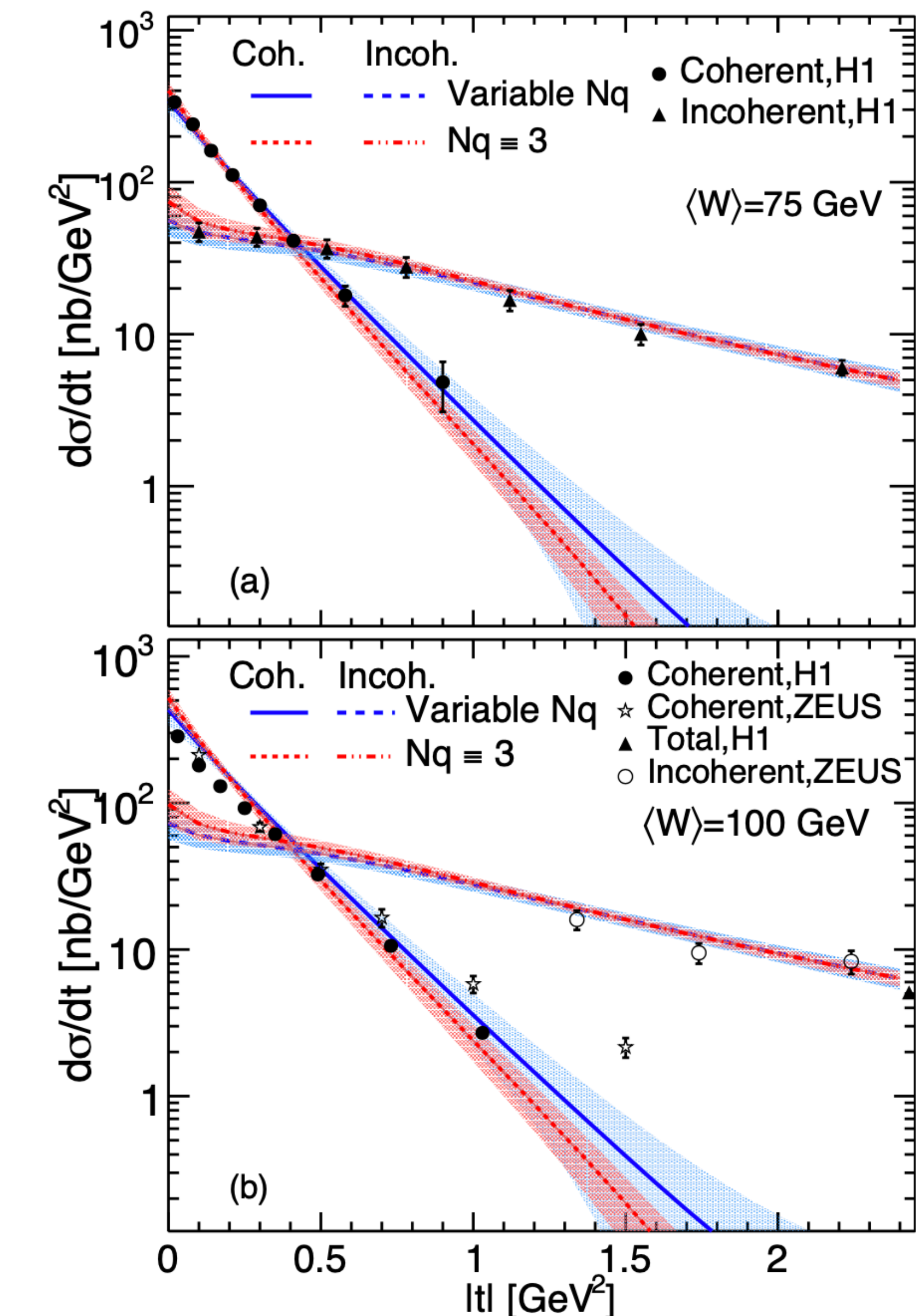
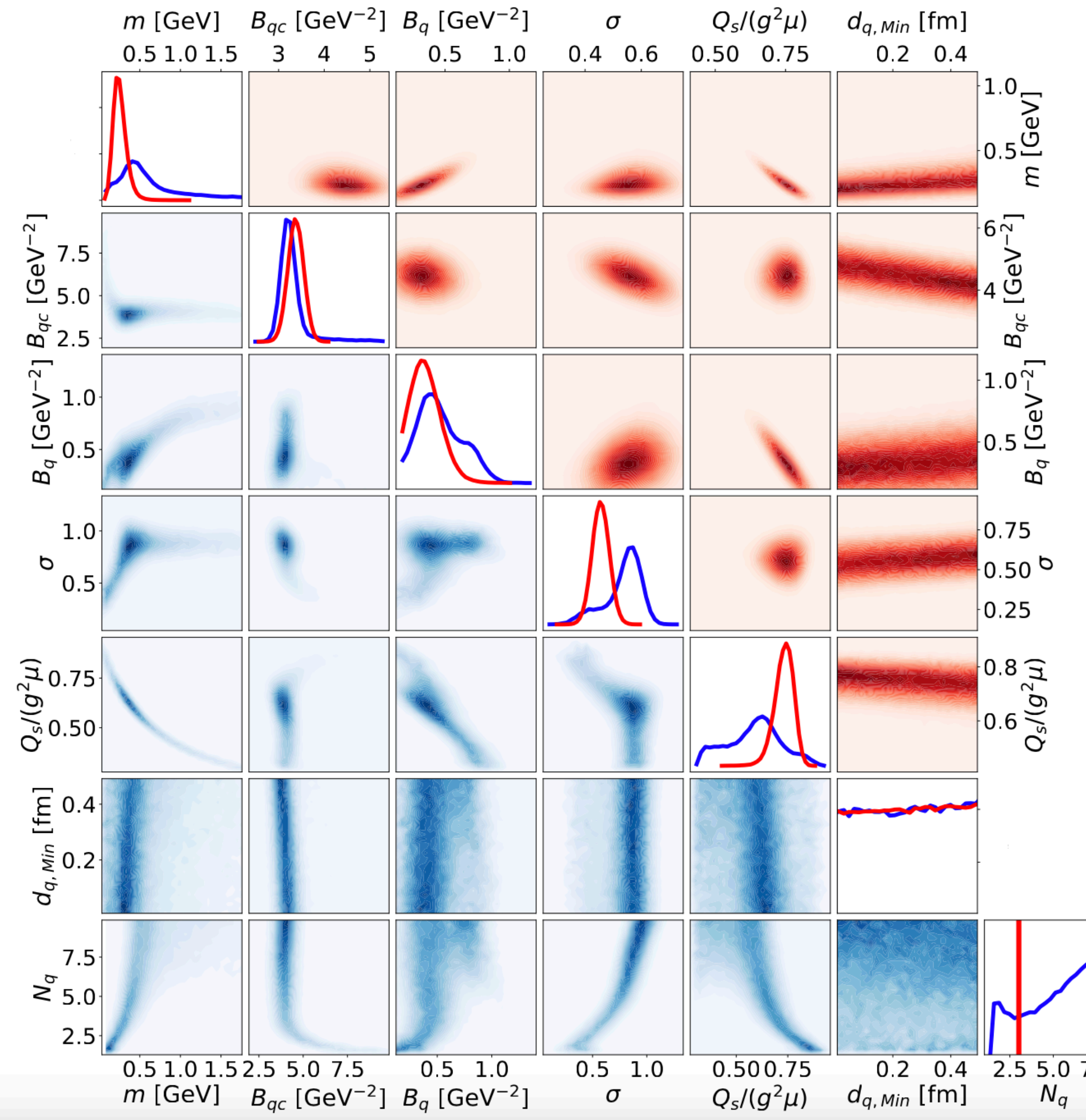
B. Schenke, Rep. Prog. Phys. 84 082301 (2021)



H1 Collaboration, Eur. Phys. J. C73 (2013) no. 6 2466

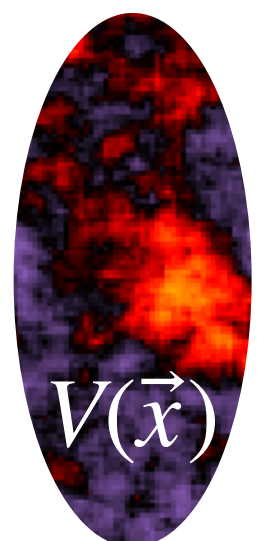
Extracting parameters using Bayesian inference

H. Mäntysaari, B. Schenke, C. Shen, W. Zhao, Phys.Lett.B 833 (2022) 137348



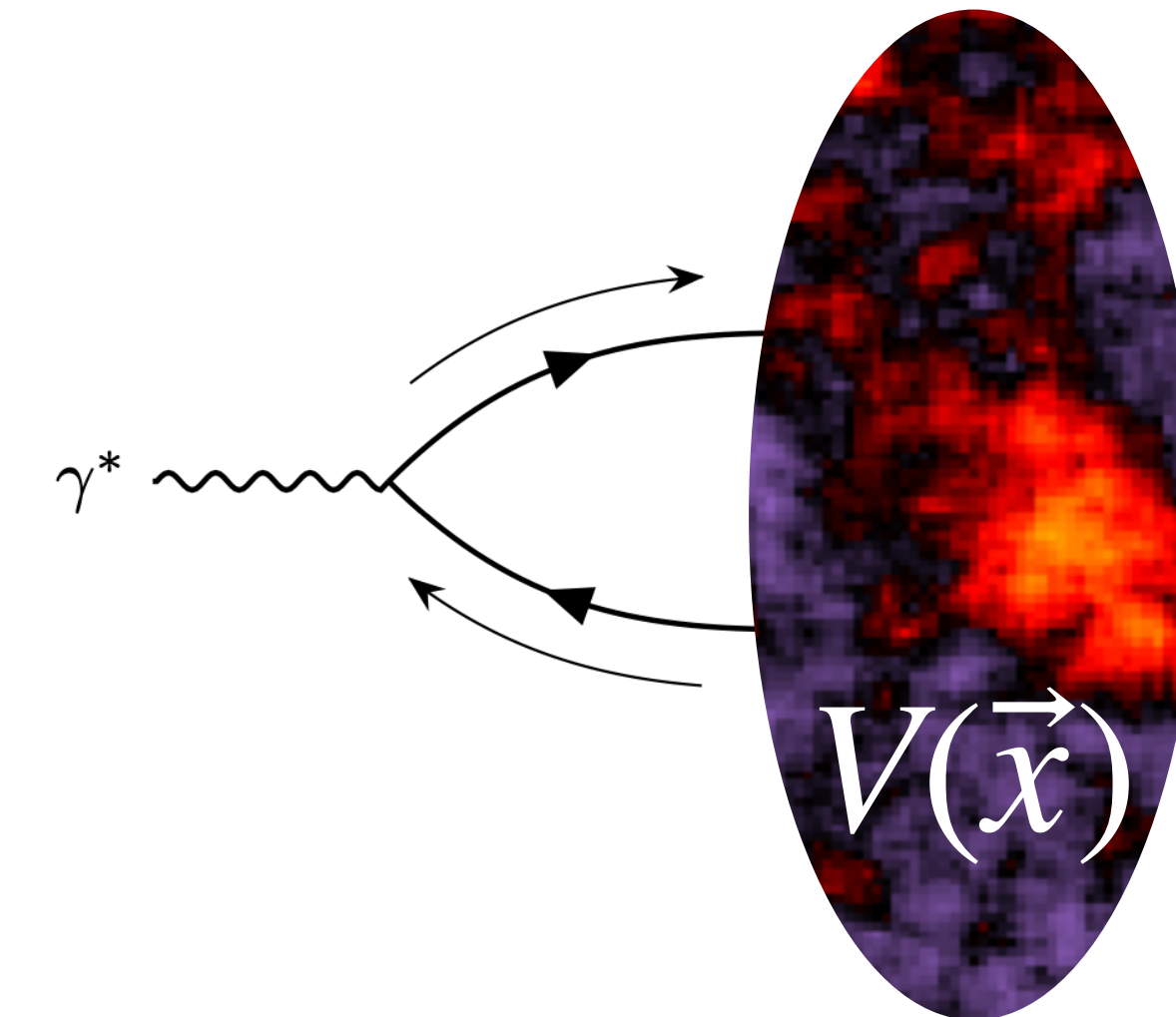
Universal Wilson lines

We use one framework to compute Wilson lines for a nucleus at a given energy.

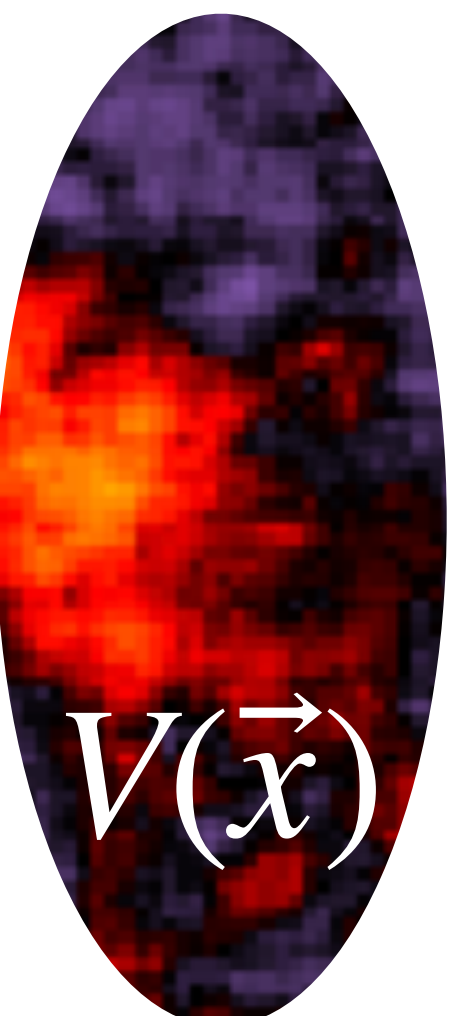
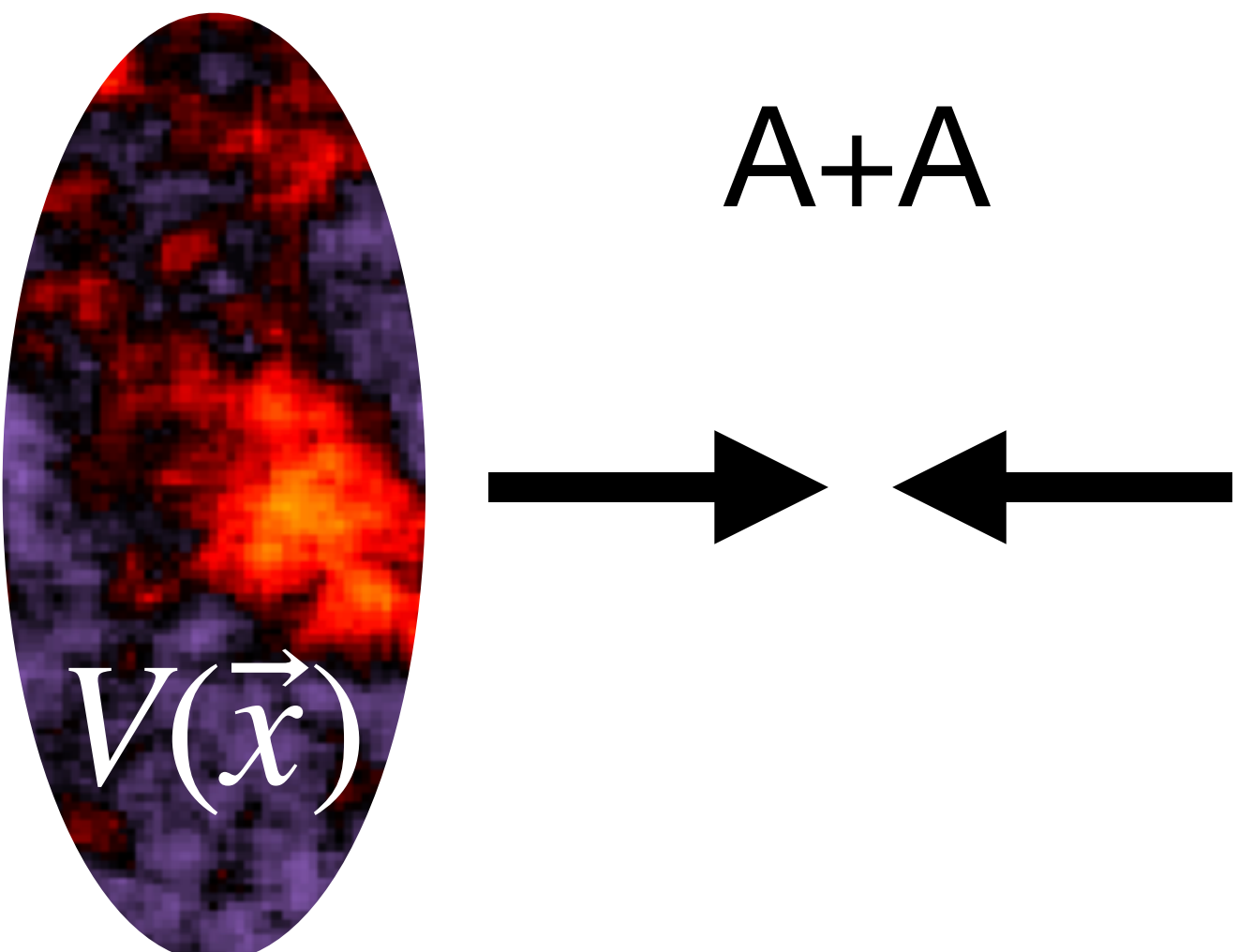


This allows to directly constrain parameters (like hot spot sizes) using one process (e.g. in $e+A$ or $e+p$) and employ the model for another (e.g. in $A+A$ or $p+A$)

$e+A$ or UPC

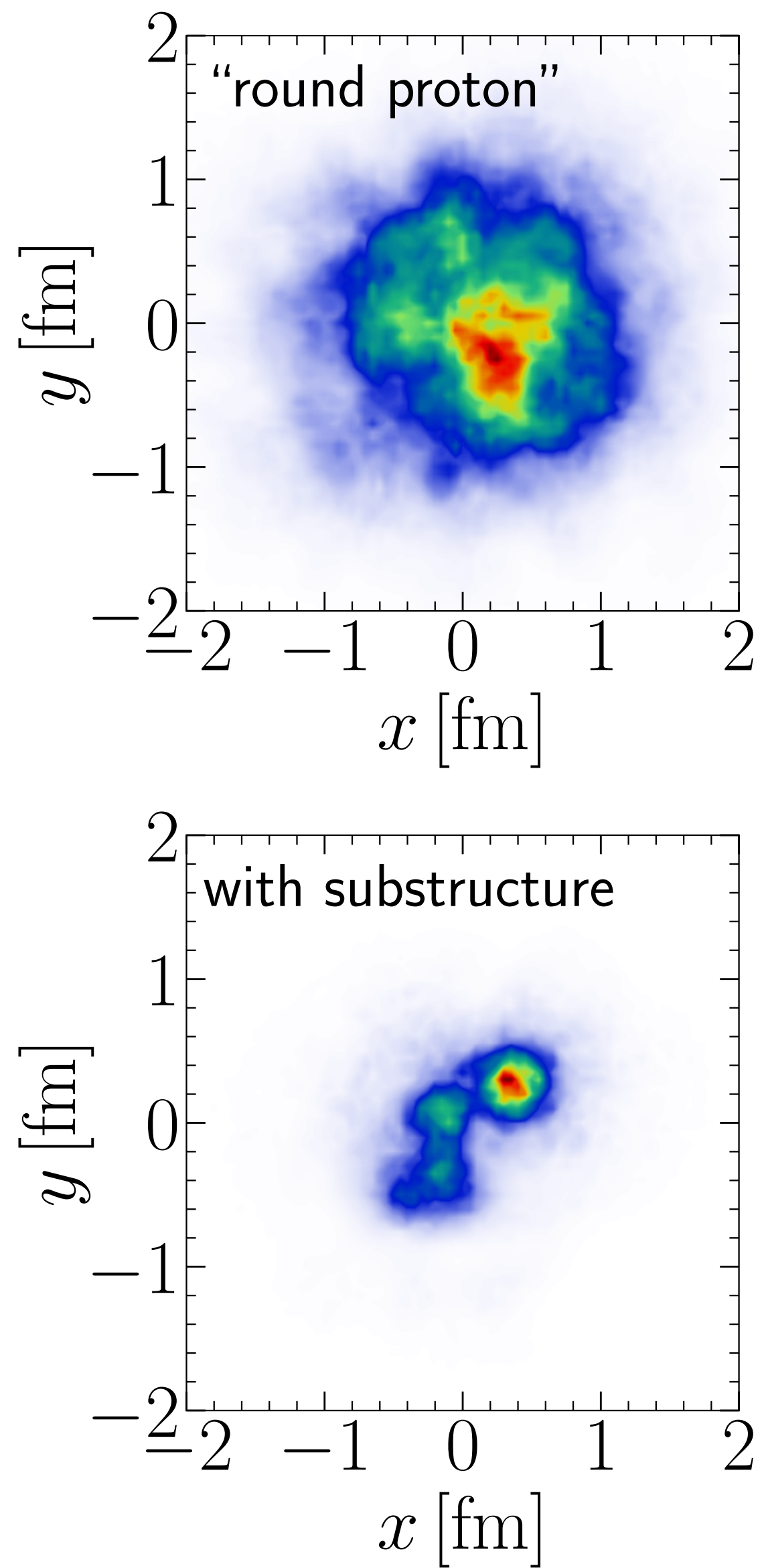
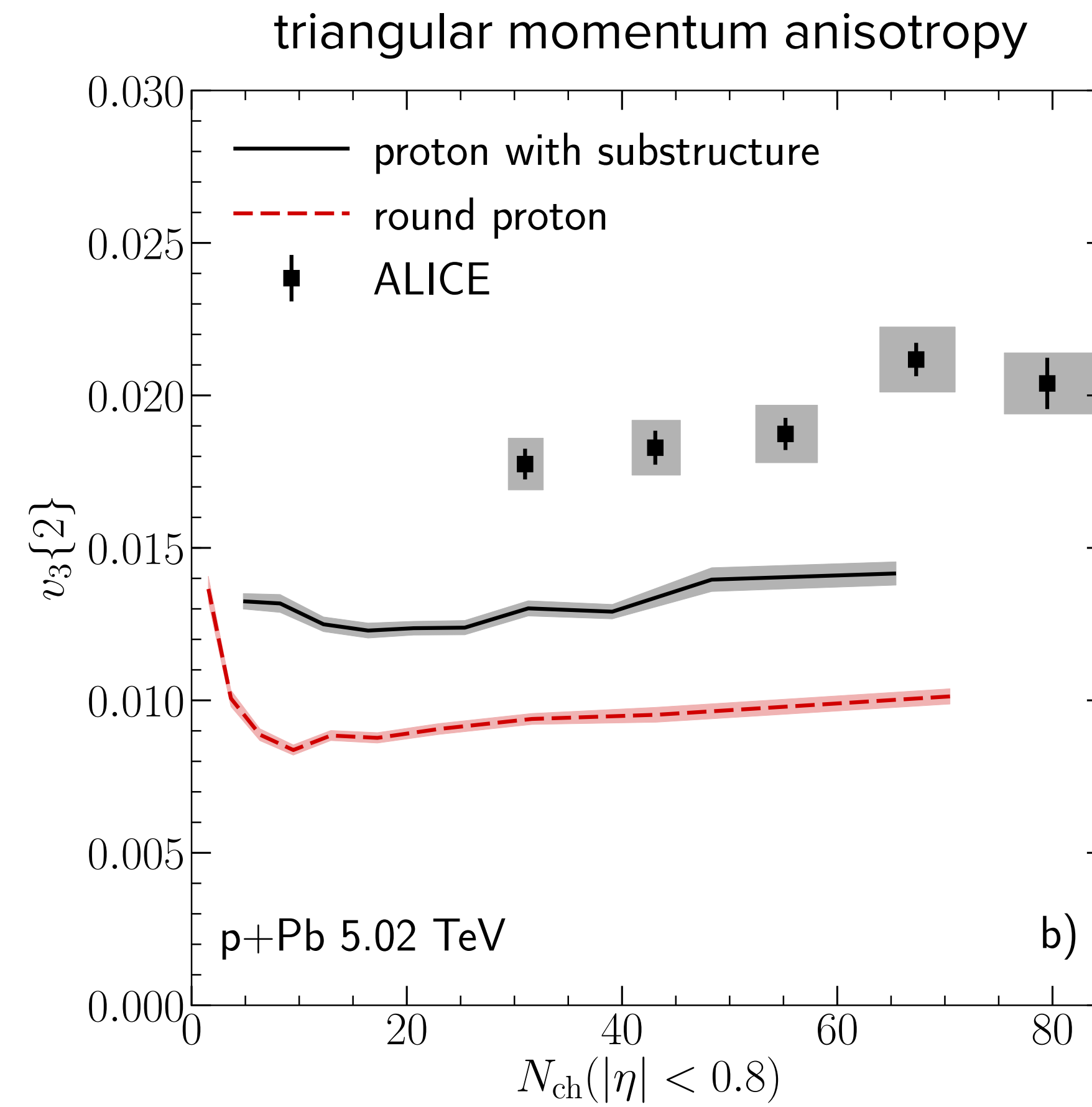
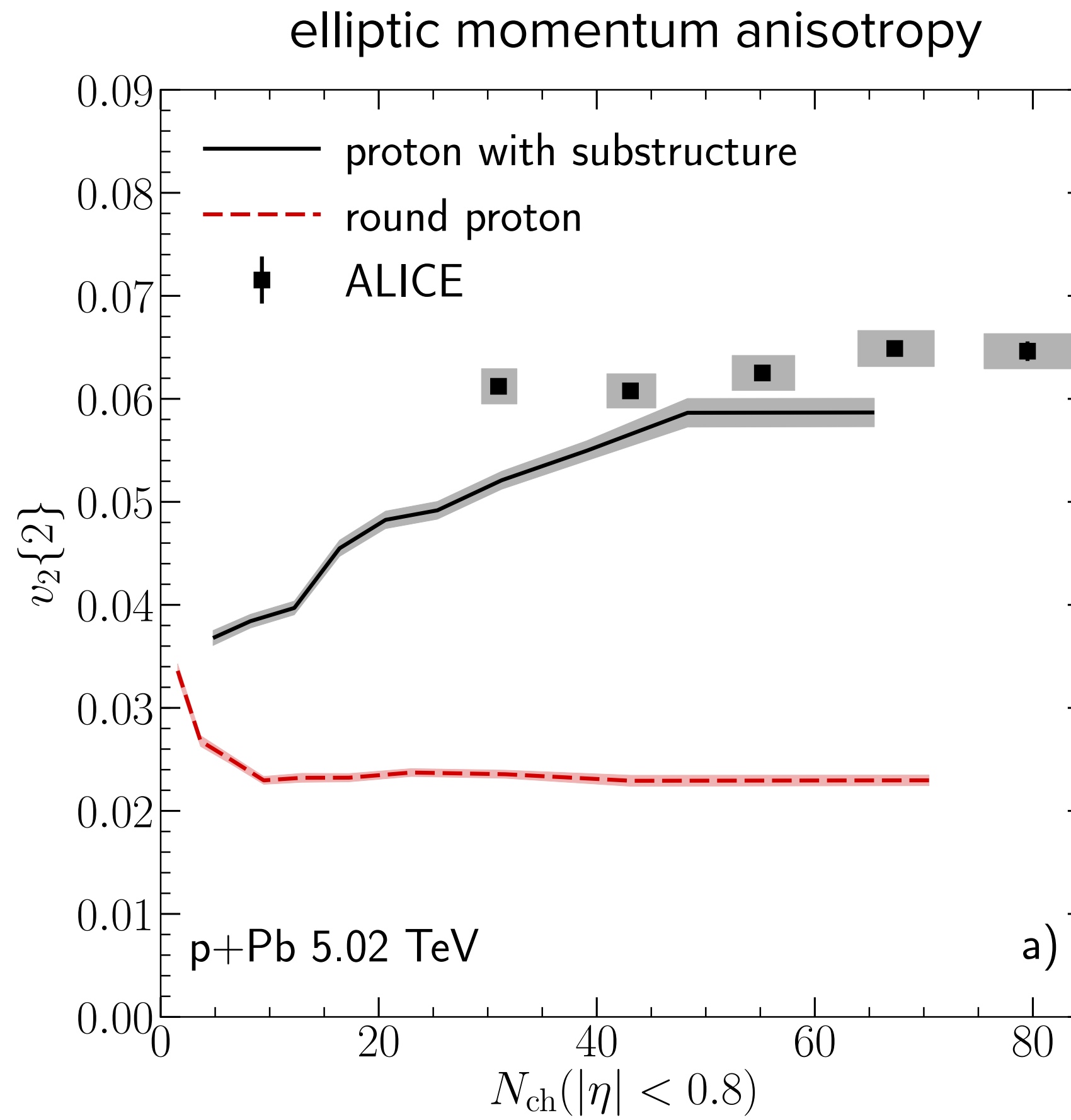


$A+A$



Consistency with p+A collisions

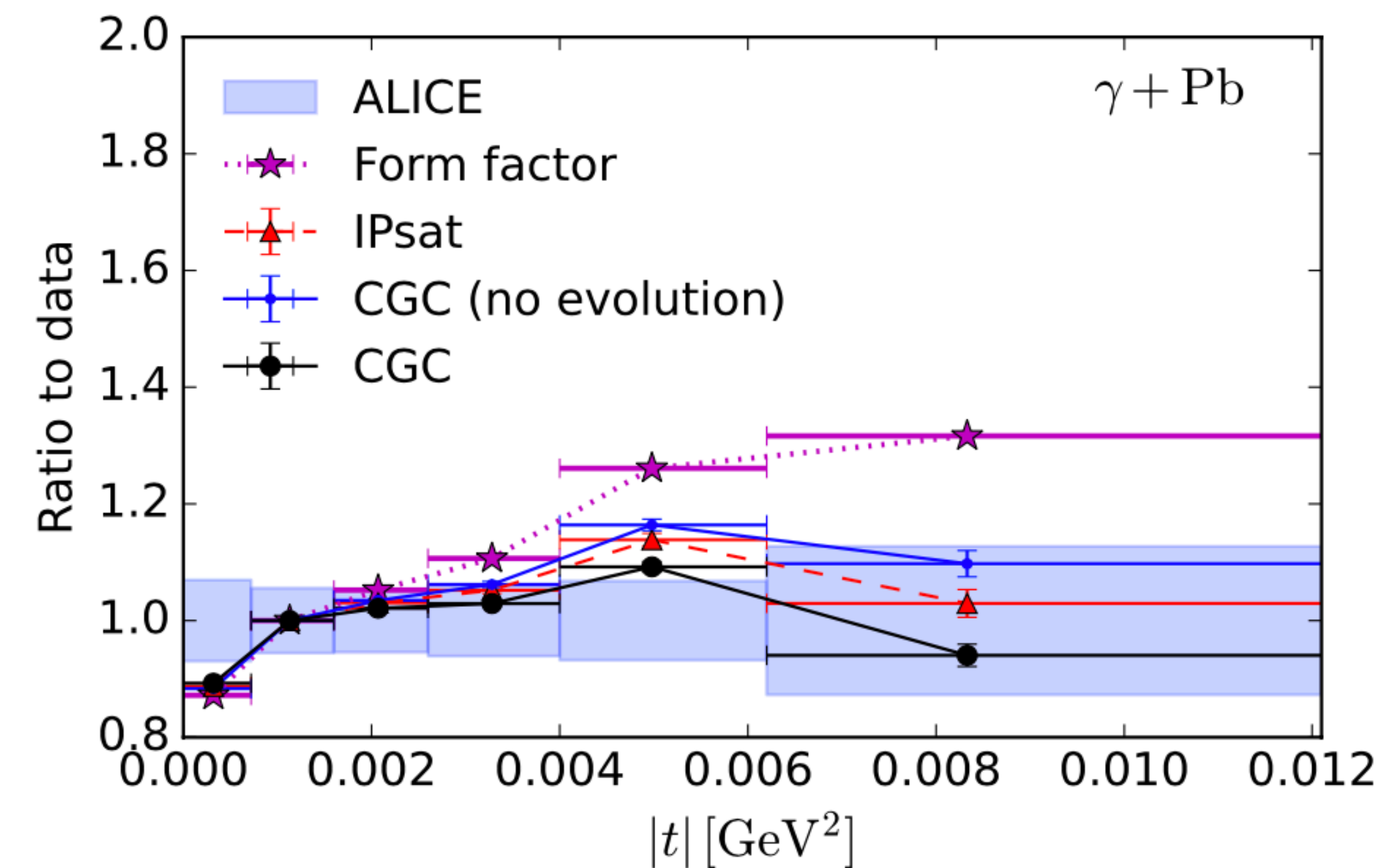
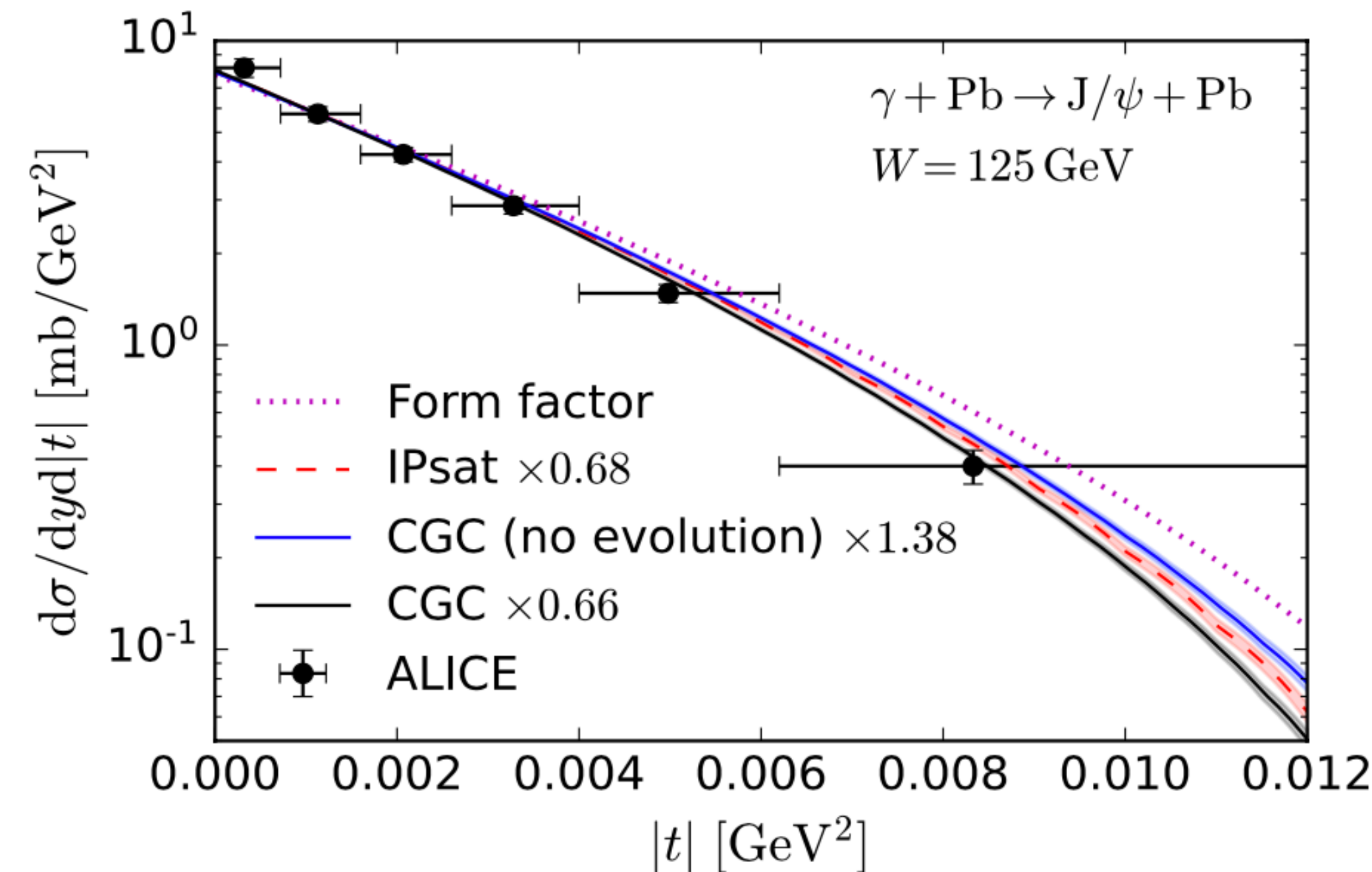
B. Schenke, Rep. Prog. Phys. 84 082301 (2021)



UPCs: γ +Pb measurement - Role of saturation effects

H. Mäntysaari, F. Salazar, B. Schenke, Phys.Rev.D 106 (2022) 7, 074019

Here, ALICE removed interference and photon k_T effects to get the γ +Pb cross section



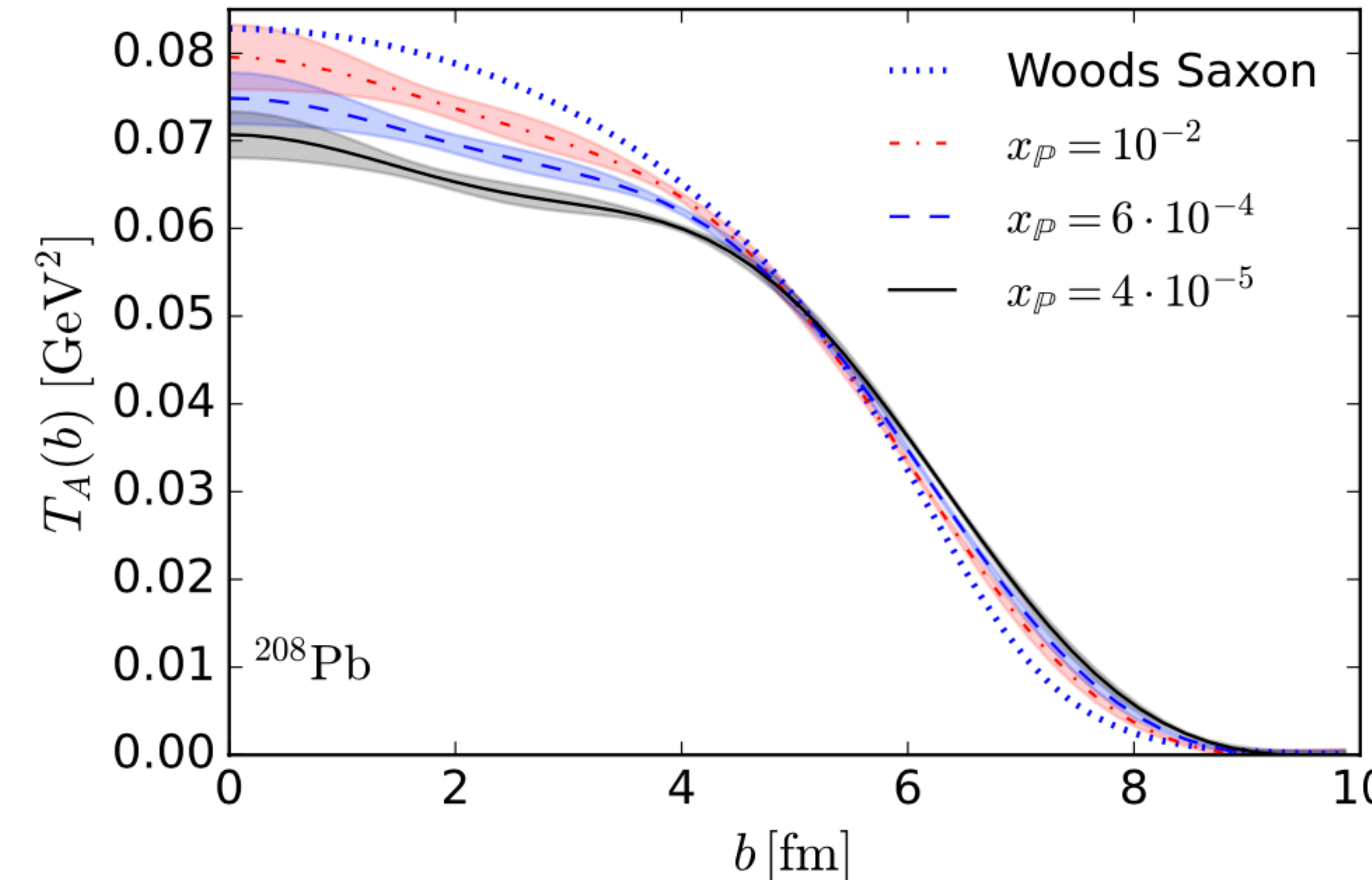
ALICE Collaboration, Phys.Lett.B 817 (2021) 136280

Saturation effects improve agreement with experimental data significantly

Saturation effects on nuclear geometry

H. Mäntysaari, F. Salazar, B. Schenke, Phys.Rev.D 106 (2022) 7, 074019

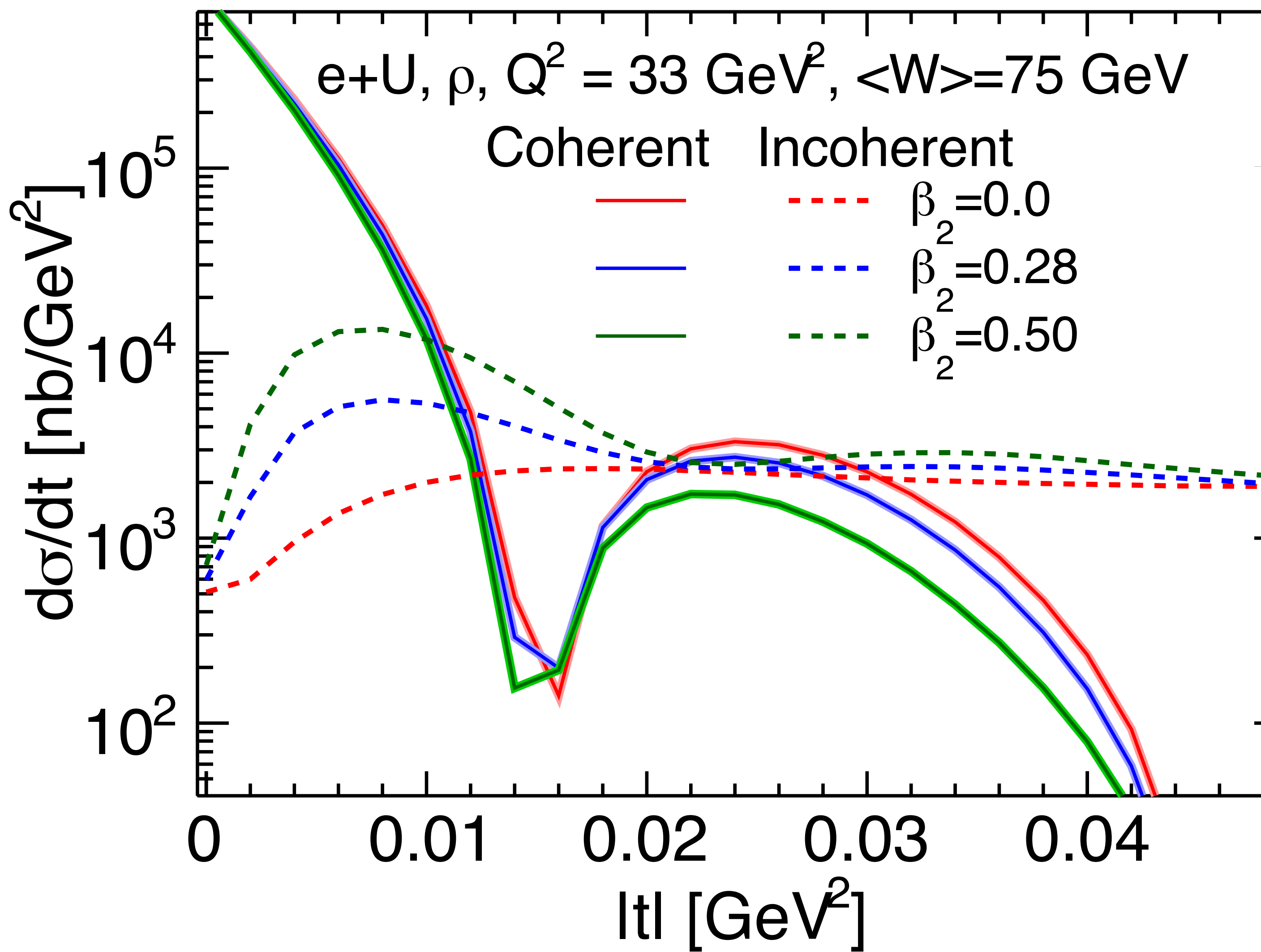
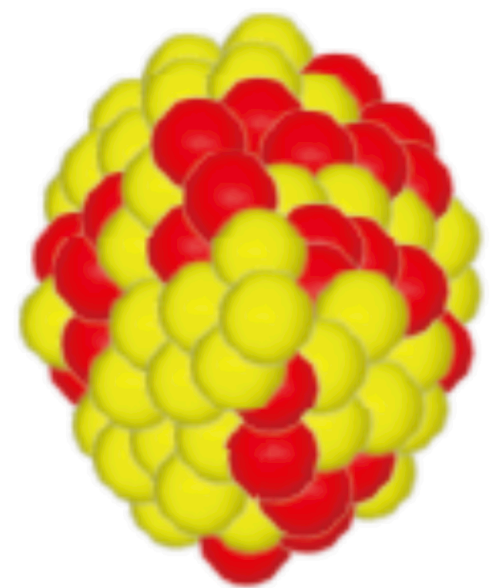
Fourier transform to coordinate space



JIMWLK evolution leads to growth of the nucleus towards small x
and depletion near the center (normalized so $\int d^2b T_A(b) = 208$)

Nuclear structure at high energy: Deformed gluon distributions?

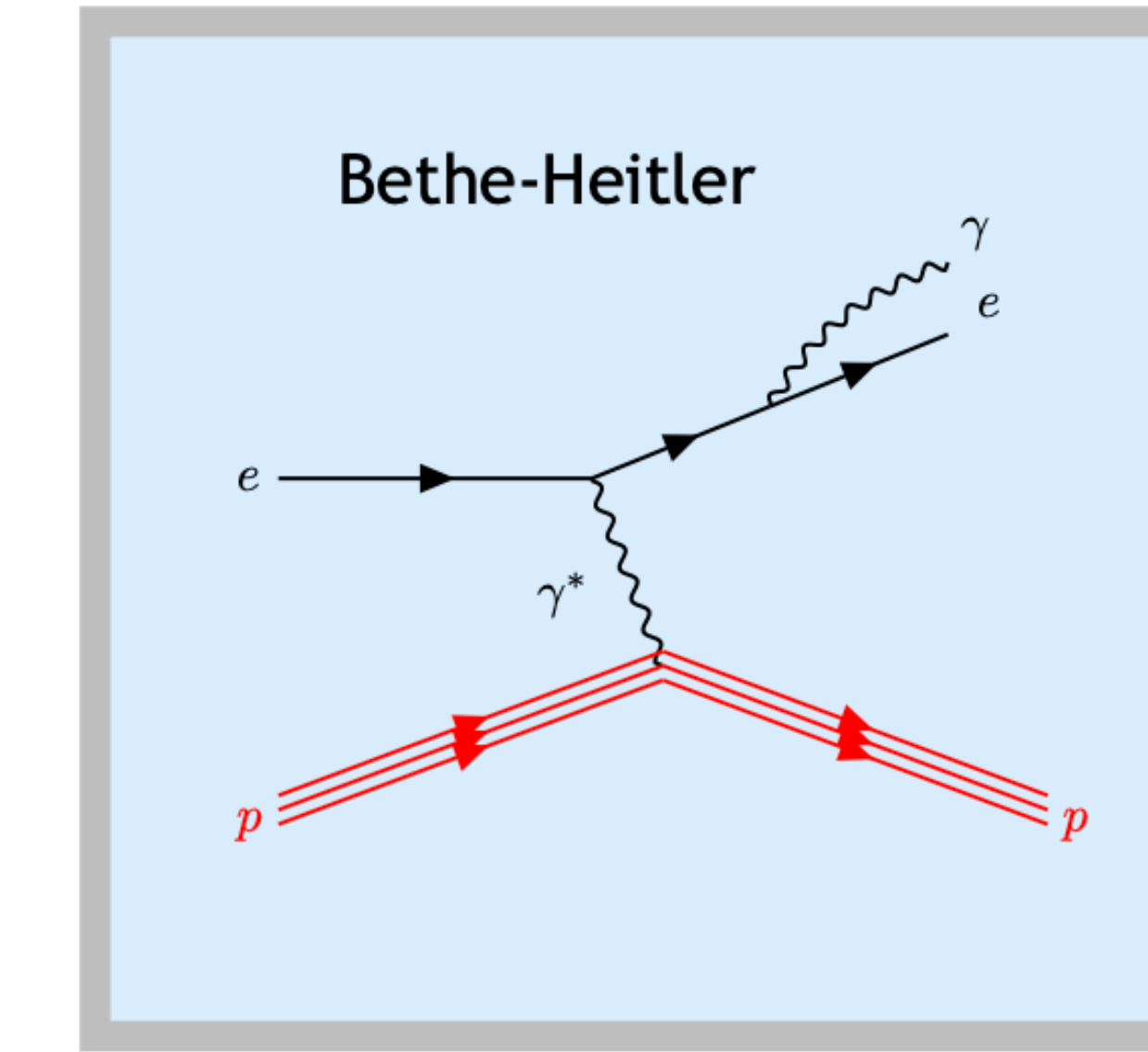
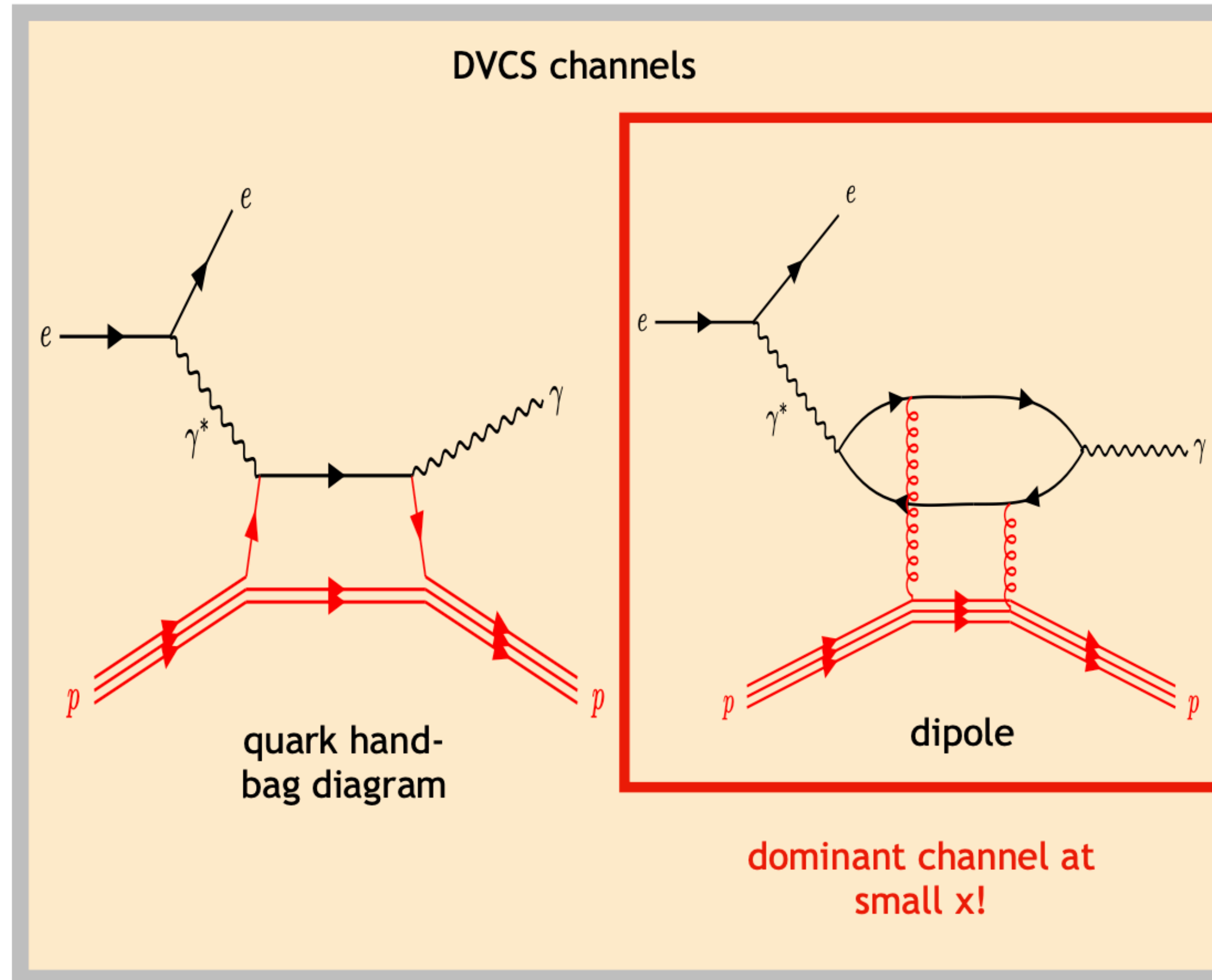
H. Mäntysaari, B. Schenke, C. Shen, W. Zhao, in progress



$$\rho(r, \theta, \phi) = \frac{\rho_0}{1 + e^{[r - R(\theta, \phi)]/a}},$$
$$R(\theta, \phi) = R_0 (1 + \beta_2 Y_2^0 + \beta_3 Y_3^0 + \beta_4 Y_4^0)$$

Deformation of the nucleus affects incoherent cross section at small $|t|$ (large length scales) and provides direct information on the nuclear structure at small x

Angular dependence in exclusive VM production and DVCS

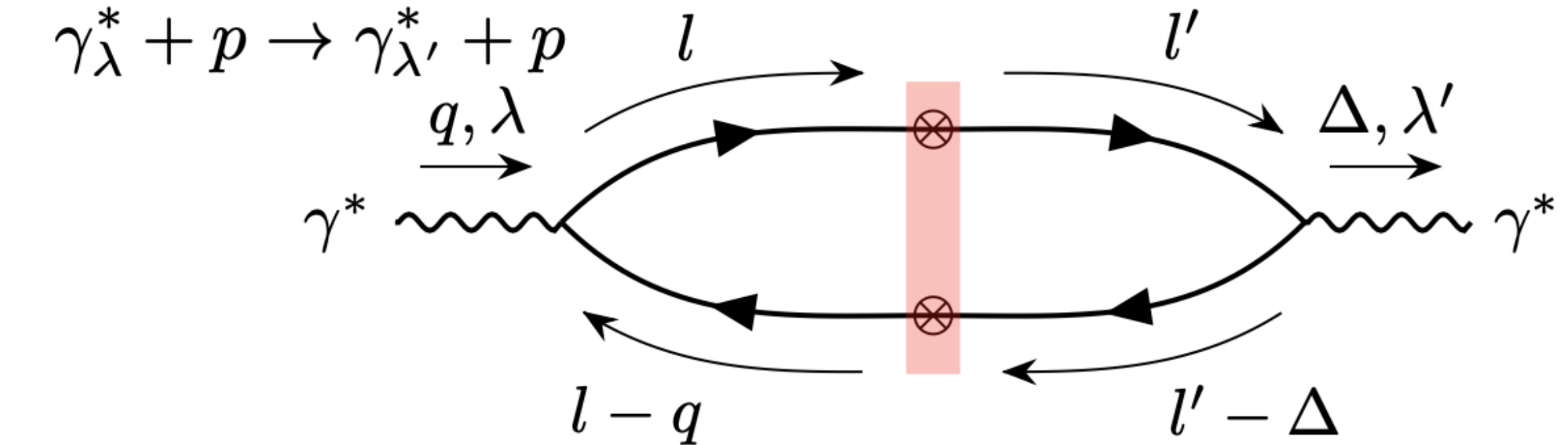
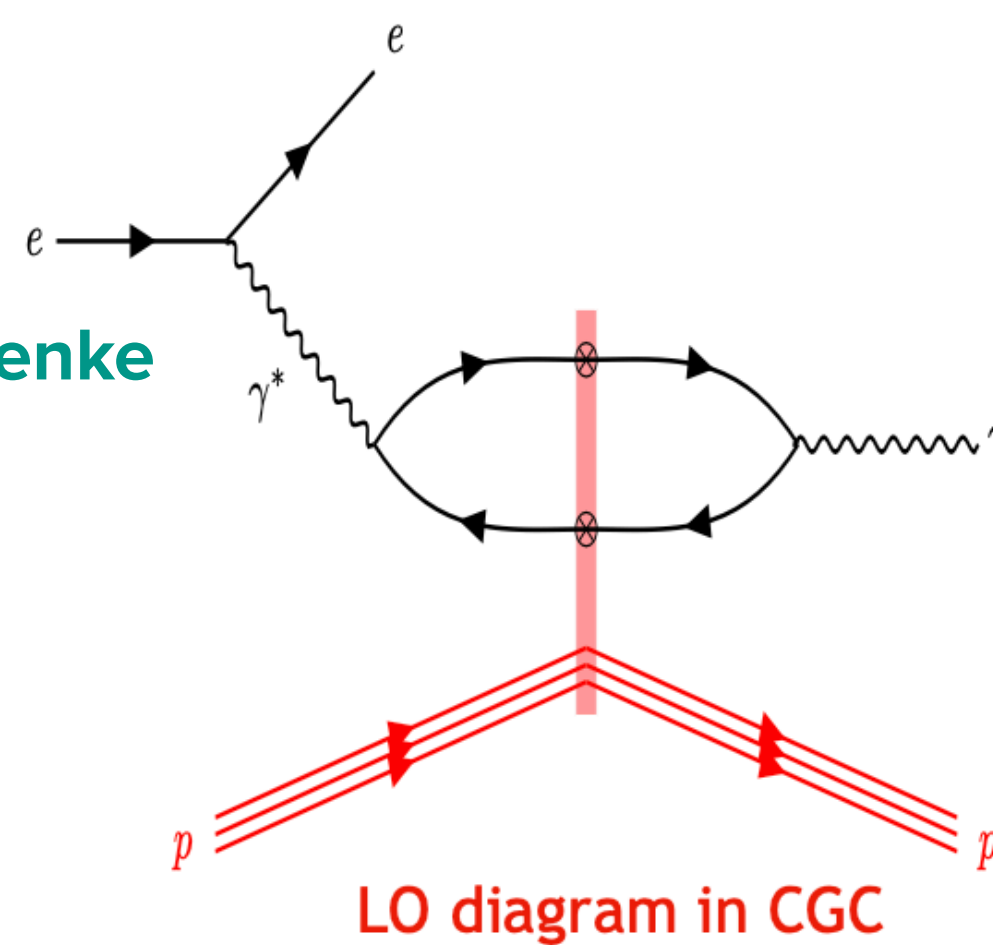


For DVCS and BH see

Aschenauer, Fazio,
Kumericki, Müller [1304.0077](#)

DVCS in the CGC

H. Mäntysaari, K. Roy, F. Salazar, B. Schenke
 Phys. Rev. D 103 (2021) 9, 094026



Helicity preserving amplitude

$$\langle \mathcal{M}_{\pm 1, \pm 1} \rangle_Y \sim \int_{\mathbf{b}_\perp} e^{-i\Delta_\perp \cdot \mathbf{b}_\perp} \int_{\mathbf{r}_\perp} D_Y(\mathbf{r}_\perp, \mathbf{b}_\perp) \int_z e^{-i\delta_\perp \cdot \mathbf{r}_\perp} [(z^2 + \bar{z}^2) \varepsilon_f K_1(\varepsilon_f r_\perp) \varepsilon'_f K_1(\varepsilon'_f r_\perp) + m_f K_0(\varepsilon_f r_\perp) m_f K_0(\varepsilon'_f r_\perp)]$$

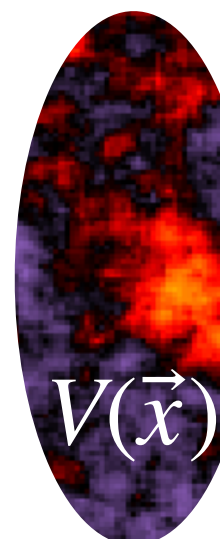
Helicity flip amplitude

$$\langle \mathcal{M}_{\pm 1, \mp 1} \rangle_Y \sim e^{\pm 2i\phi_\Delta} \int_{\mathbf{b}_\perp} e^{-i\Delta_\perp \cdot \mathbf{b}_\perp} \int_{\mathbf{r}_\perp} e^{\pm 2i\phi_{r\Delta}} D_Y(\mathbf{r}_\perp, \mathbf{b}_\perp) \int_z e^{-i\delta_\perp \cdot \mathbf{r}_\perp} z\bar{z} \varepsilon_f K_1(\varepsilon_f r_\perp) \varepsilon'_f K_1(\varepsilon'_f r_\perp)$$

Similar expressions for other amplitudes: $\langle \mathcal{M}_{0,0} \rangle_Y$ $\langle \mathcal{M}_{\pm 1,0} \rangle_Y$ $\langle \mathcal{M}_{0,\pm 1} \rangle_Y$

$$D_Y(\mathbf{r}_\perp, \mathbf{b}_\perp) = 1 - \frac{1}{N_c} \left\langle \text{Tr} \left[V \left(\mathbf{b}_\perp + \frac{\mathbf{r}_\perp}{2} \right) V^\dagger \left(\mathbf{b}_\perp - \frac{\mathbf{r}_\perp}{2} \right) \right] \right\rangle_Y$$

Again, the same Wilson lines

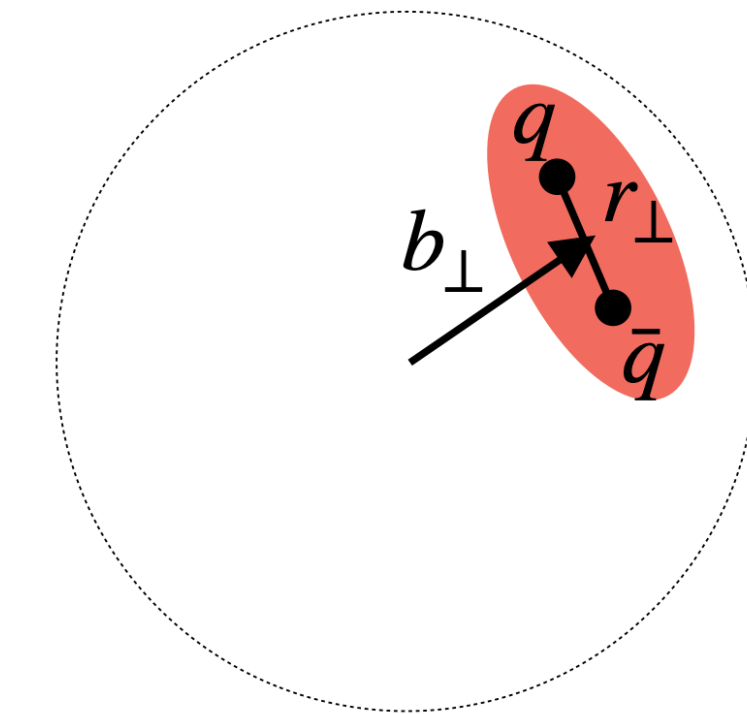
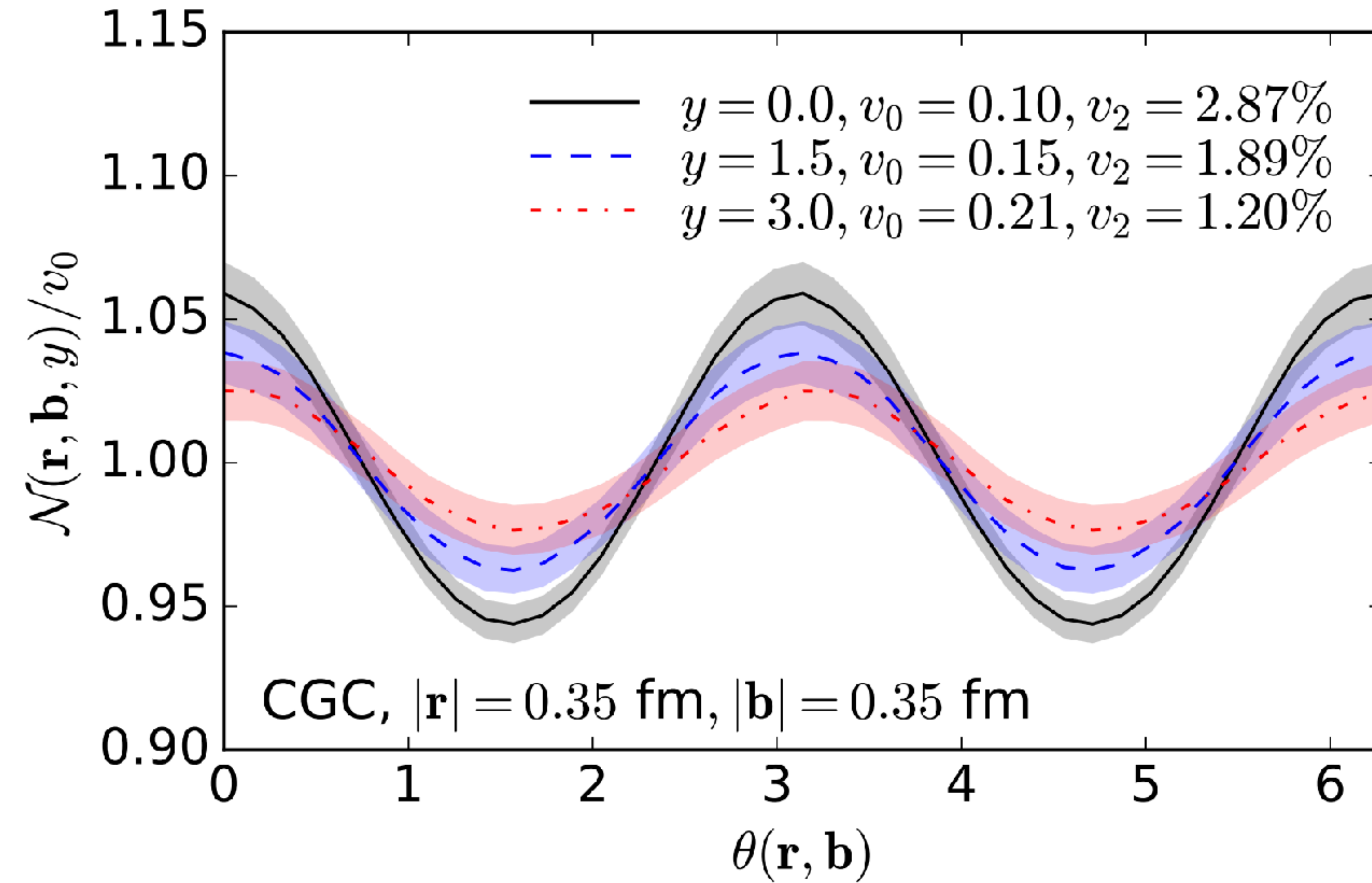


$$\delta_\perp = \left(\frac{z - \bar{z}}{2} \right) \Delta_\perp$$

Anisotropy in the angle between impact parameter and dipole orientation

H. Mäntysaari, N. Mueller, B. Schenke, Phys. Rev. D 99, 074004 (2019)

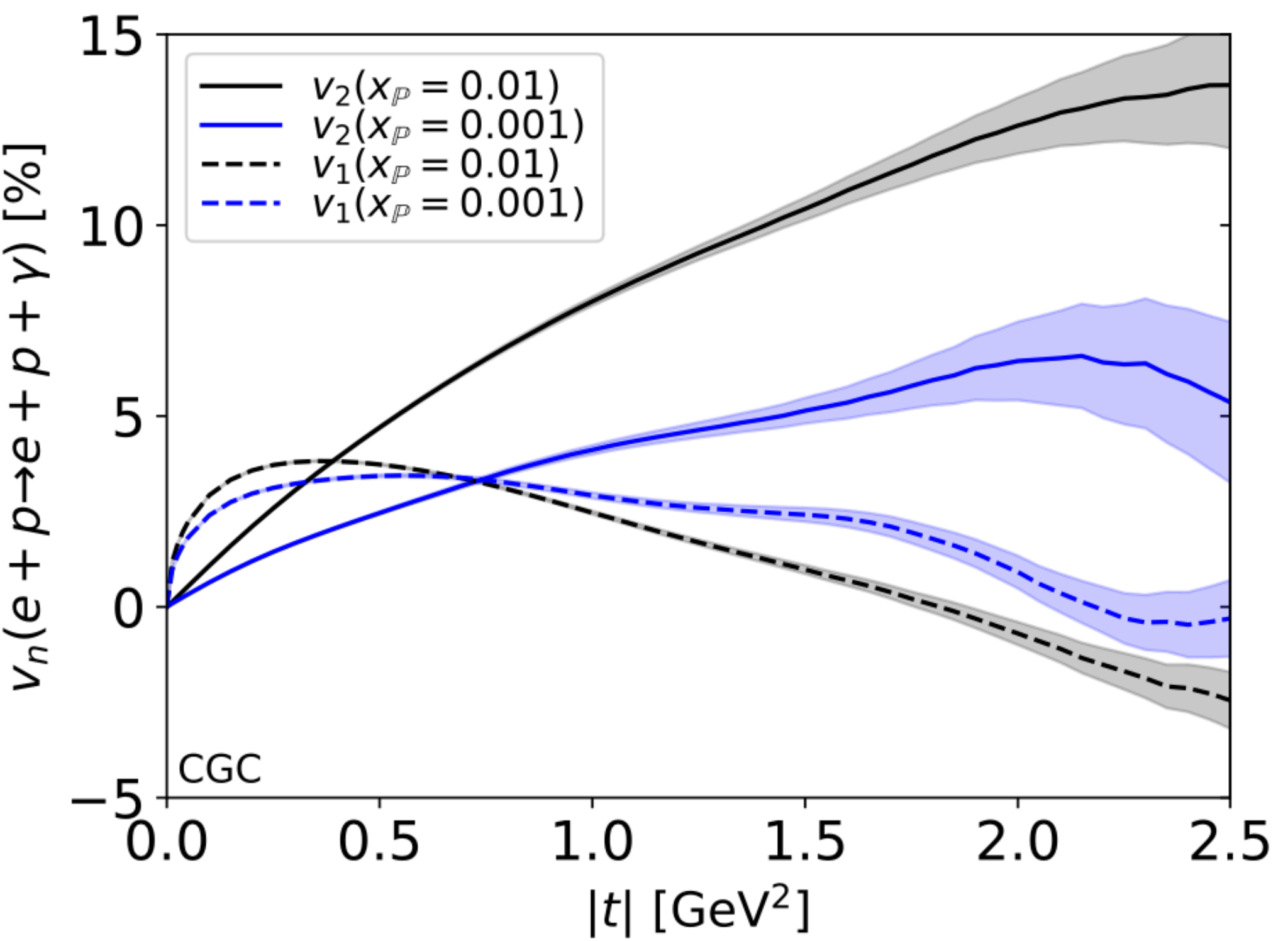
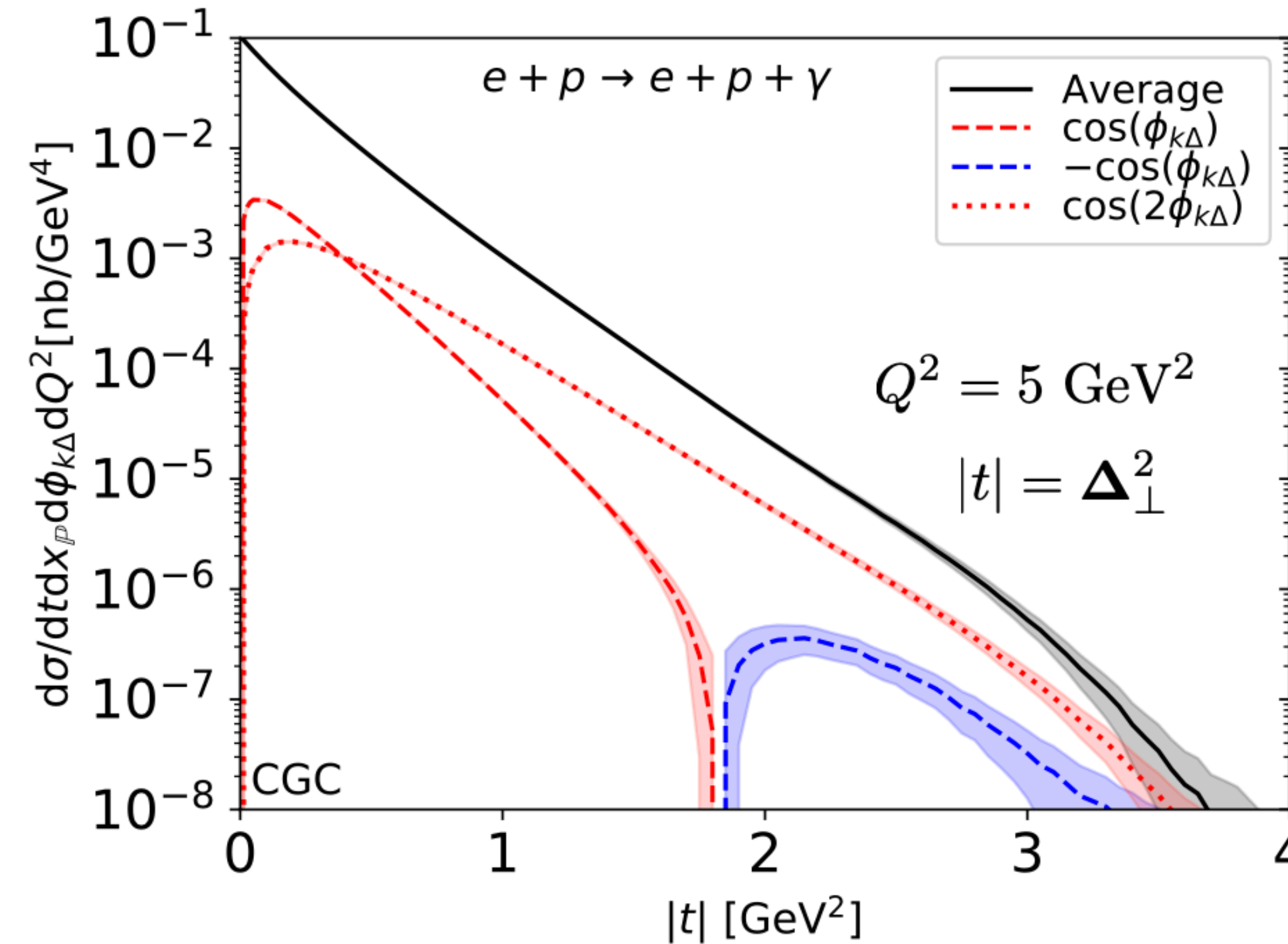
Anisotropy in the dipole amplitude: $D_Y = \mathcal{N}(\mathbf{r}, \mathbf{b}, x) = v_0 [1 + 2v_2 \cos(2\theta(\mathbf{r}, \mathbf{b}))]$



DVCS in e+p with angular dependence in the CGC

H. Mäntysaari, K. Roy, F. Salazar, B. Schenke, Phys.Rev.D 103 (2021) 9, 094026

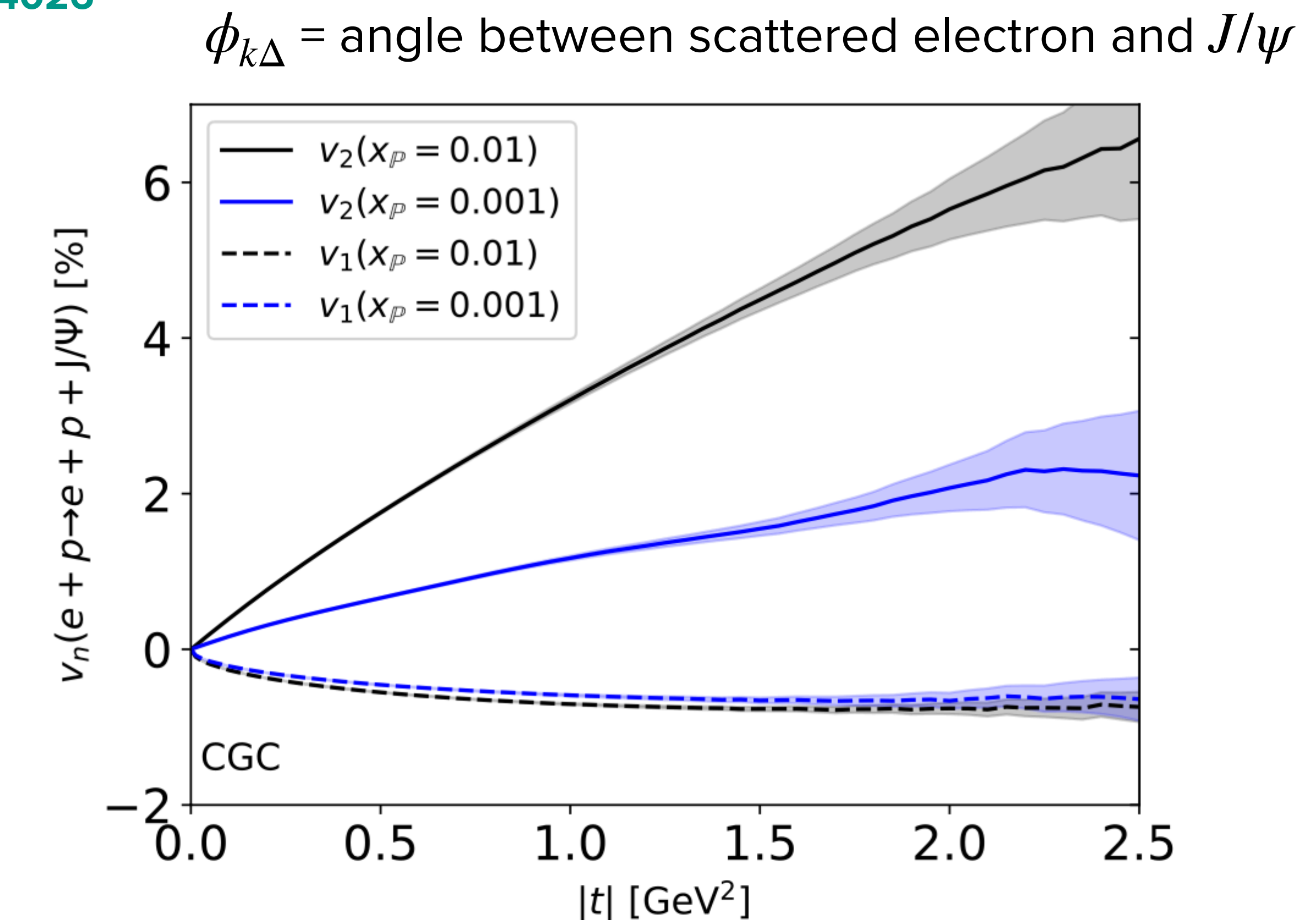
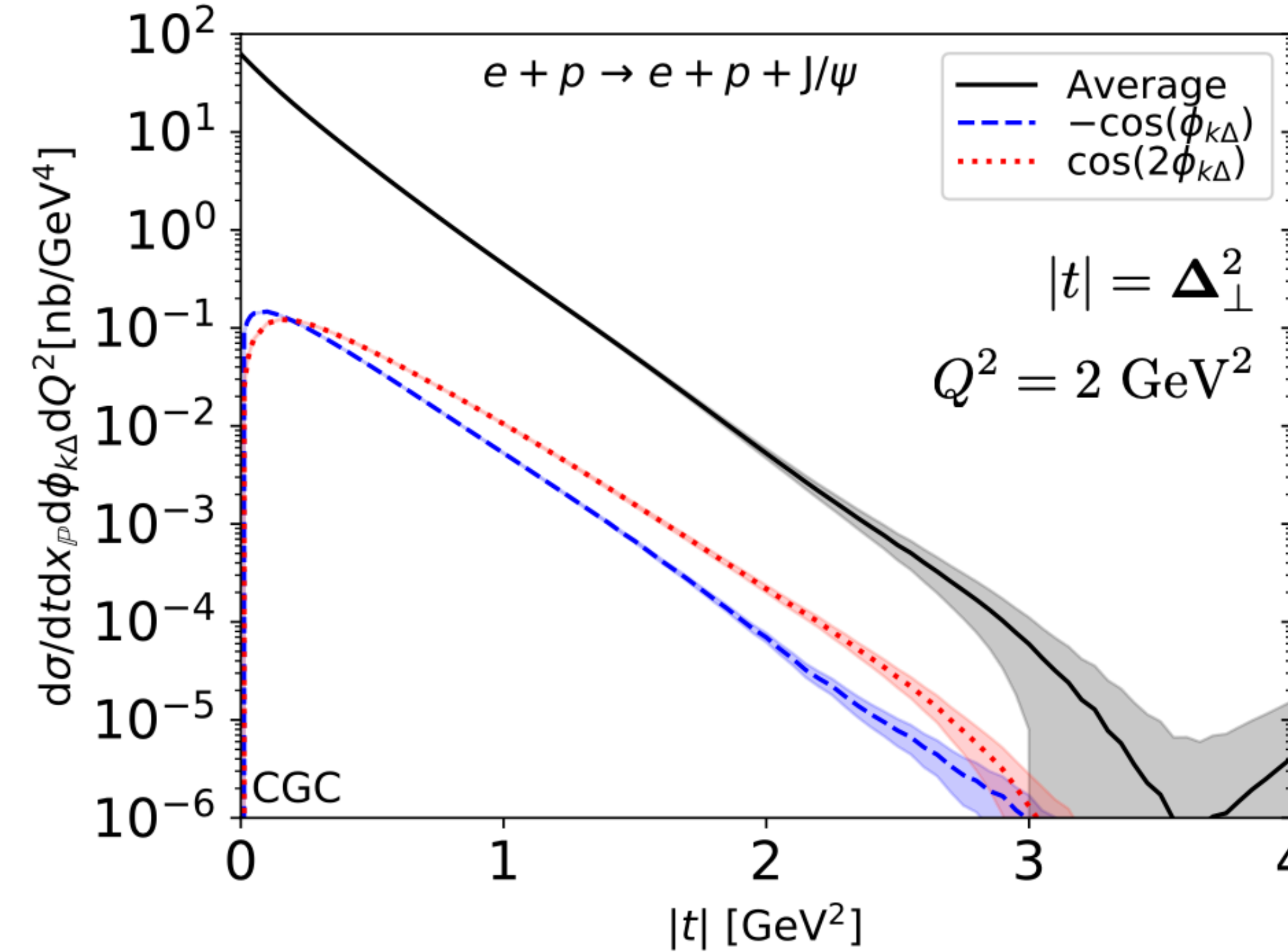
$\phi_{k\Delta}$ = angle between scattered electron and photon



Significant contribution from large dipoles even at large Q^2 due to $z \rightarrow 0,1$

J/ψ production in e+p with angular dependence in the CGC

H. Mäntysaari, K. Roy, F. Salazar, B. Schenke, Phys.Rev.D 103 (2021) 9, 094026



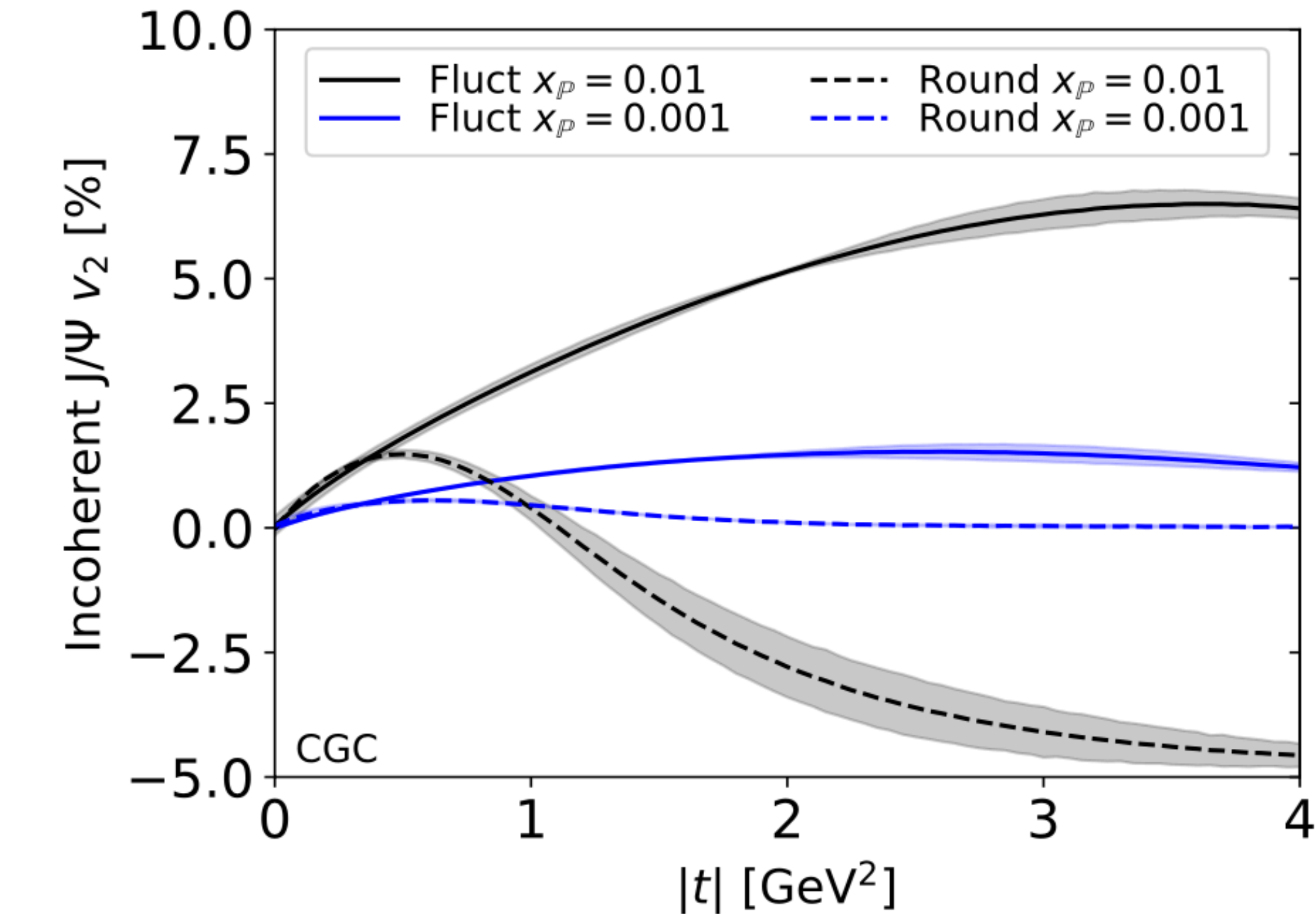
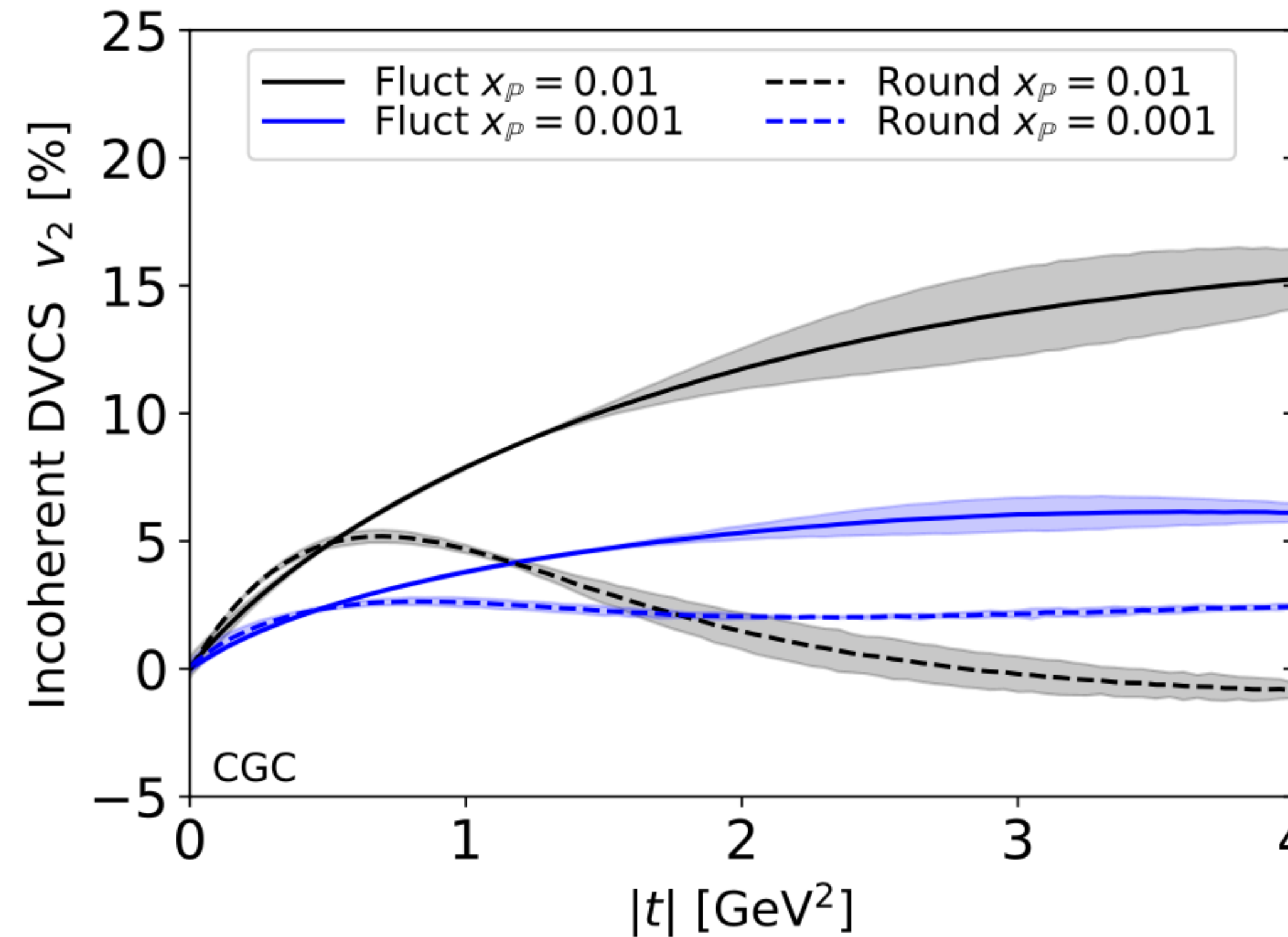
Sizeable azimuthal anisotropies (a few percent) which decrease with small- x evolution

Color charge gradients drive azimuthal anisotropy

Incoherent diffraction and fluctuations

DVCS and J/ψ correlation with electron plane

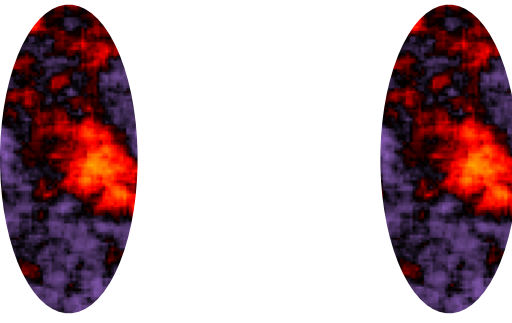
H. Mäntysaari, K. Roy, F. Salazar, B. Schenke, Phys.Rev.D 103 (2021) 9, 094026



Substructure fluctuations change anisotropies at moderate momentum transfer
 $|t| \gtrsim 0.5 \text{ GeV}^2$, increasing v_2

Connection to GPDs

Hatta, Yuan, Xiao. 1703.02085



FT to momentum space: $F_x(q_\perp, \Delta_\perp) = \int \frac{d^2 r_\perp d^2 b_\perp}{(2\pi)^4} e^{ib_\perp \cdot \Delta_\perp + ir_\perp \cdot q_\perp} S_x \left(b_\perp + \frac{r_\perp}{2}, b_\perp - \frac{r_\perp}{2} \right)$

Isotropic and elliptic parts: $F_x(q_\perp, \Delta_\perp) = F_0(|q_\perp|, |\Delta_\perp|) + 2 \cos 2(\phi_{q_\perp} - \phi_{\Delta_\perp}) F_\epsilon(|q_\perp|, |\Delta_\perp|) + \dots$

GPDs are defined via $\frac{1}{P^+} \int \frac{d\zeta^-}{2\pi} e^{ixP^+\zeta^-} \langle p' | F^{+i}(-\zeta/2) F^{+j}(\zeta/2) | p \rangle$

$$= \frac{\delta^{ij}}{2} x H_g(x, \Delta_\perp) + \frac{x E_{Tg}(x, \Delta_\perp)}{2M^2} \left(\Delta_\perp^i \Delta_\perp^j - \frac{\delta^{ij} \Delta_\perp^2}{2} \right) + \dots$$

Yoshitaka Hatta, Bo-Wen Xiao, Feng Yuan, Phys. Rev. Lett. 116, 202301 (2016)

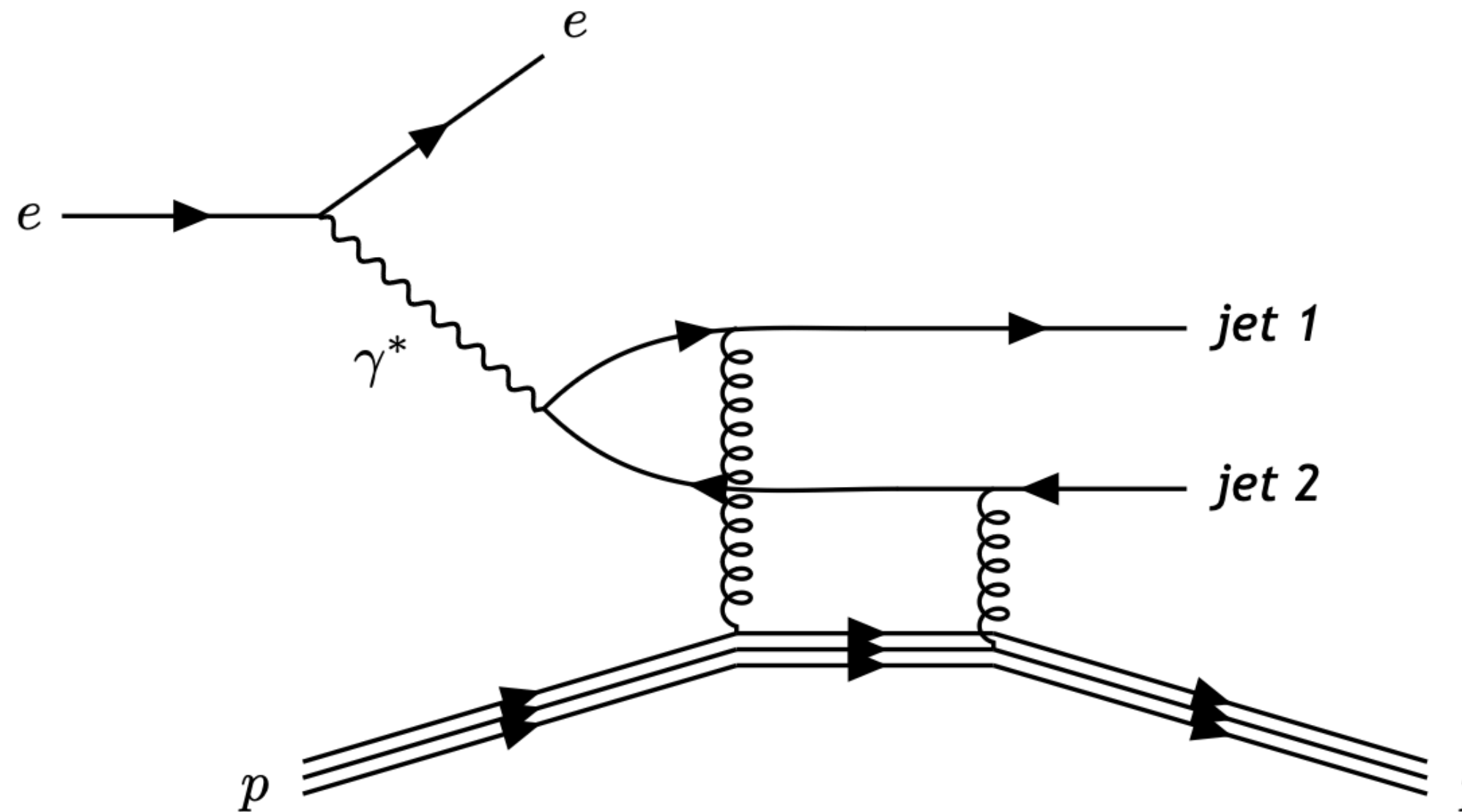
At small x one can show $\frac{1}{P^+} \int \frac{d\zeta^-}{2\pi} e^{ixP^+\zeta^-} \langle p' | F^{+i} F^{+j} | p \rangle \approx \frac{2N_c}{\alpha_s} \int d^2 q_\perp \left(q_\perp^i - \frac{\Delta_\perp^i}{2} \right) \left(q_\perp^j + \frac{\Delta_\perp^j}{2} \right) F_x(q_\perp, \Delta_\perp)$

Then:

$$x H_g(x, \Delta_\perp) = \frac{2N_c}{\alpha_s} \int d^2 q_\perp q_\perp^2 F_0, \quad x E_{Tg}(x, \Delta_\perp) = \frac{4N_c M^2}{\alpha_s \Delta_\perp^2} \int d^2 q_\perp q_\perp^2 F_\epsilon$$

Diffractive dijet production

Accessing the Dipole gluon GTMD at the EIC



Exclusive dijet electro-production

Hatta, Yuan, Xiao (2016)
Mäntysaari, Mueller, Schenke (2019)
FS, Schenke (2019)

At EIC energies, the small- x constrain
the invariant mass of dijet system

$\rightarrow p_\perp \lesssim 5$ GeV

Challenging to reconstruct
experimentally

Include effects of soft-gluon radiation

\rightarrow Better to measure recoiled
target

Hatta, Mueller, Ueda, Yuan (2019)
Hatta, Yuan, Xiao, Zhou (2020)

Maybe worth studying heavy quark pair via charm fragmentation function $c \rightarrow D$

Accessing GTMD at small x and $Q^2 \approx 0$

Y. Hagiwara, Y. Hatta, R. Pasechnik, M. Tasevsky, O. Teryaev, Phys. Rev. D 96, 034009 (2017)

$$xW(x, \vec{q}_\perp, \vec{\Delta}_\perp) \approx \frac{2N_c}{\alpha_s} \left(q_\perp^2 - \frac{\Delta_\perp^2}{4} \right) S_Y(\vec{q}_\perp, \vec{\Delta}_\perp)$$

Y. Hatta, B. W. Xiao and F. Yuan, Phys. Rev. Lett. 116, no. 20, 202301 (2016)

where $S_Y(\vec{q}_\perp, \vec{\Delta}_\perp) = \int \frac{d^2\vec{r}_\perp d^2\vec{b}_\perp}{(2\pi)^4} e^{i\vec{\Delta}_\perp \cdot \vec{b}_\perp + i\vec{q}_\perp \cdot \vec{r}_\perp} \left\langle \frac{1}{N_c} \text{Tr} U \left(\vec{b}_\perp + \frac{\vec{r}_\perp}{2} \right) U^\dagger \left(\vec{b}_\perp - \frac{\vec{r}_\perp}{2} \right) \right\rangle_Y$

Diffractive dijet cross section in UPC p+A for $Q^2 \approx 0$:

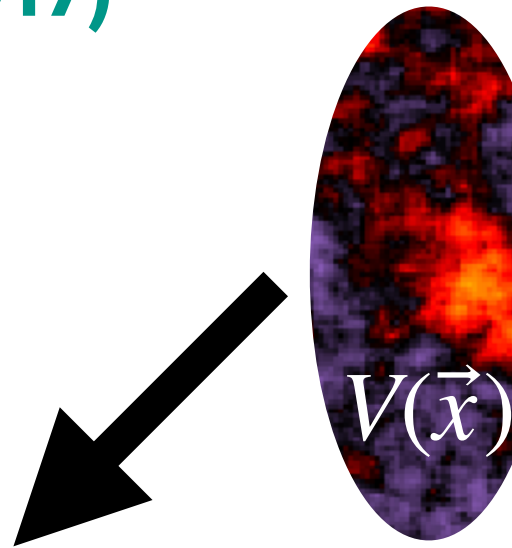
$$\frac{d\sigma^{pA}}{dy_1 dy_2 d^2\vec{k}_{1\perp} d^2\vec{k}_{2\perp}} \approx \omega \frac{dN}{d\omega} \frac{2(2\pi)^4 N_c \alpha_{em}}{P_\perp^2} \sum_f e_f^2 z (1-z) (z^2 + (1-z)^2) (A^2 + 2 \cos 2(\phi_P - \phi_\Delta) AB)$$

Measure A and B, reconstruct S: $S(\vec{q}_\perp, \vec{\Delta}_\perp) = S_0(q_\perp, \Delta_\perp) + 2 \cos 2(\phi_q - \phi_\Delta) \tilde{S}(q_\perp, \Delta_\perp)$

$$S_0(P_\perp, \Delta_\perp) = -\frac{1}{P_\perp} \frac{\partial}{\partial P_\perp} A(P_\perp, \Delta_\perp)$$

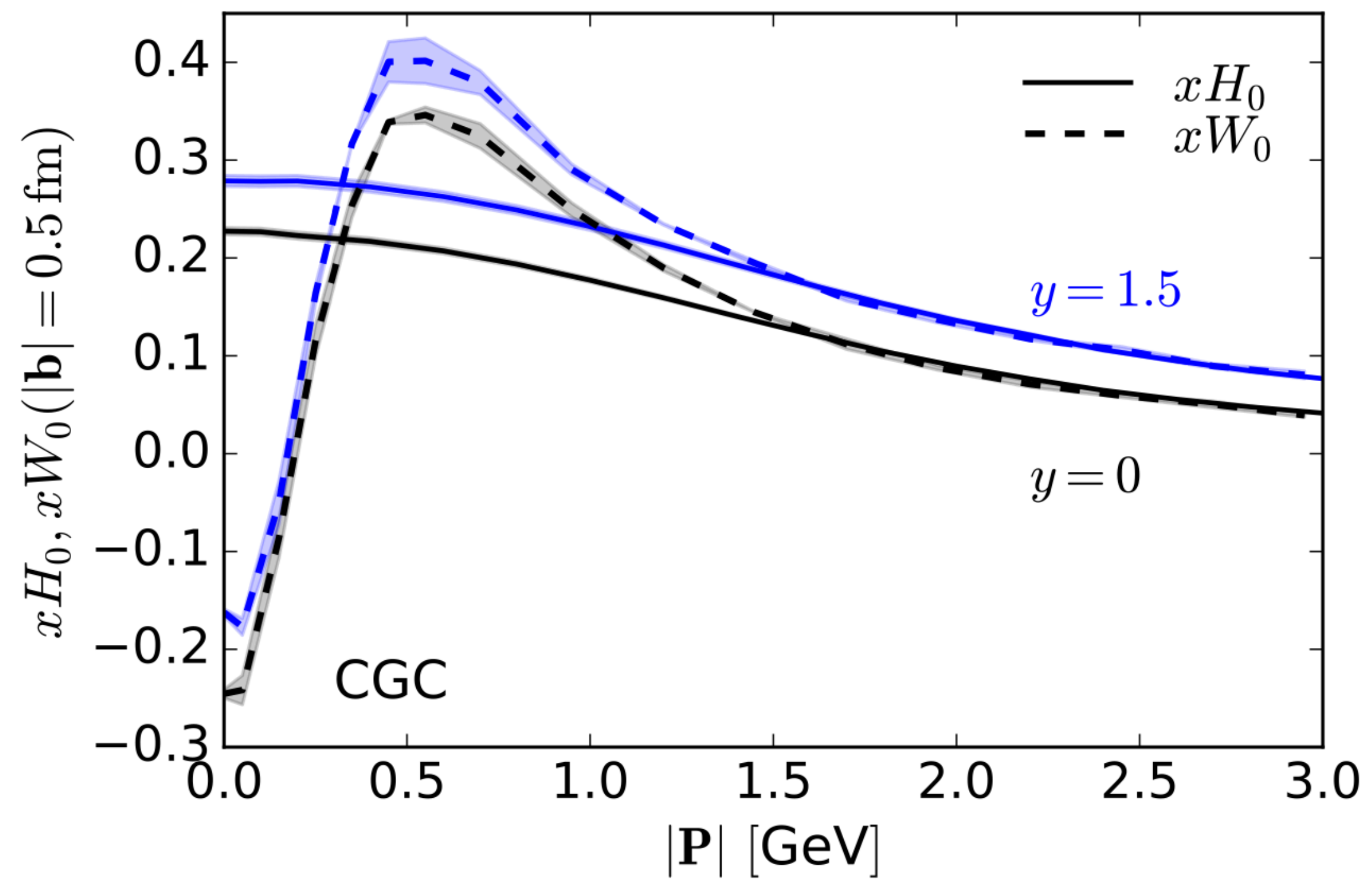
$$\tilde{S}(P_\perp, \Delta_\perp) = -\frac{\partial B(P_\perp, \Delta_\perp)}{\partial P_\perp^2} + \frac{2}{P_\perp^2} \int_0^{P_\perp^2} \frac{dP'^2_\perp}{P'^2_\perp} B(P'_\perp, \Delta_\perp)$$

$$\begin{aligned} \vec{k}_{1\perp} + \vec{k}_{2\perp} &= -\vec{\Delta}_\perp \\ \vec{P}_\perp &= \frac{1}{2}(\vec{k}_{2\perp} - \vec{k}_{1\perp}) \end{aligned}$$

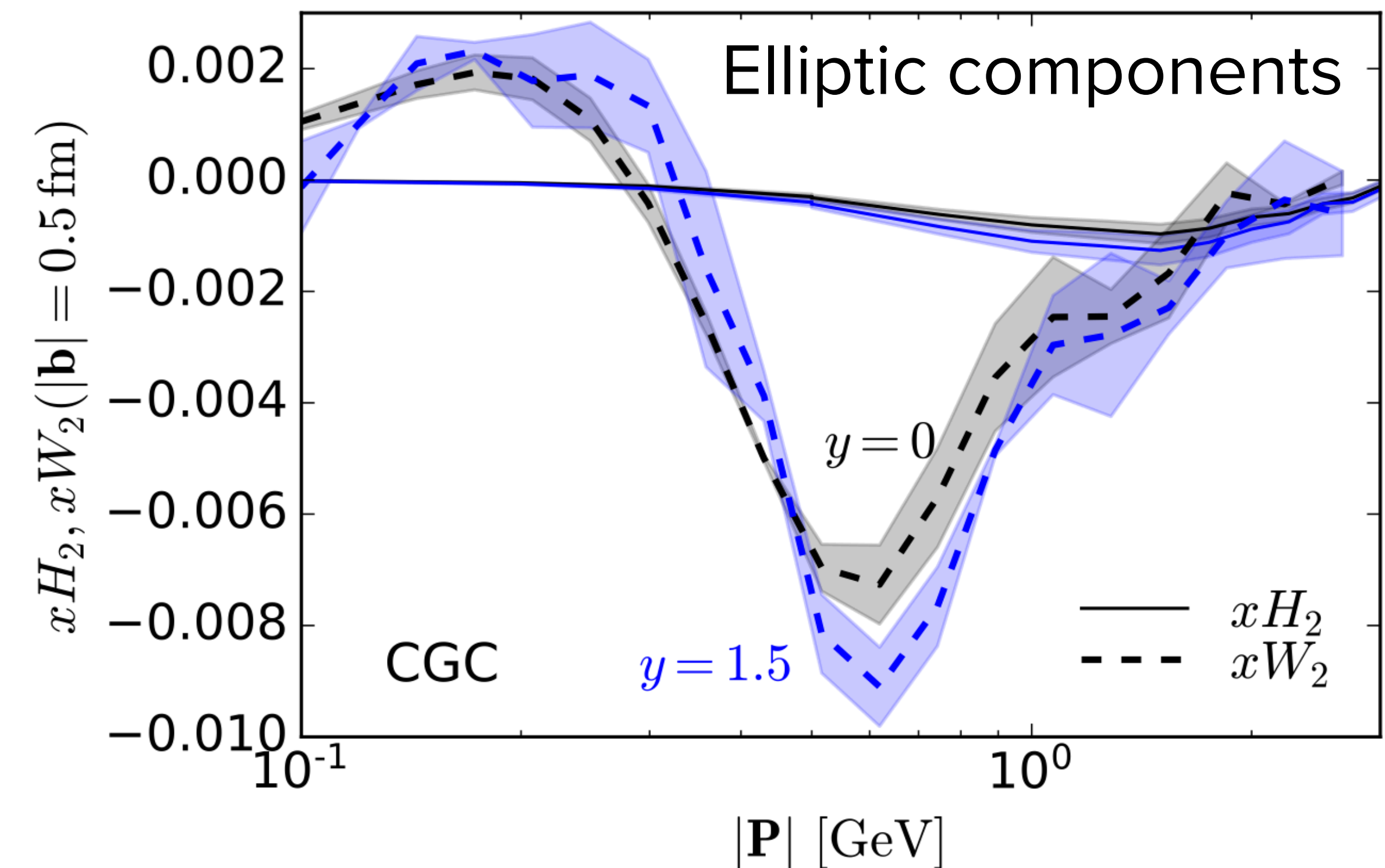


Wigner and Husimi distribution from the CGC

Numerical evaluation of xW



$$xW(\mathbf{P}, \mathbf{b}, x) = xW_0 + 2xW_2 \cos(2\theta(\mathbf{P}, \mathbf{b}))$$
$$xH(\mathbf{P}, \mathbf{b}, x) = xH_0 + 2xH_2 \cos(2\theta(\mathbf{P}, \mathbf{b}))$$



Azimuthal anisotropies in the Wigner distribution are reflected in anisotropy of the diffractive dijet cross sections H. Mäntysaari, N. Müller, B. Schenke, Phys.Rev.D 99 (2019) 7, 074004

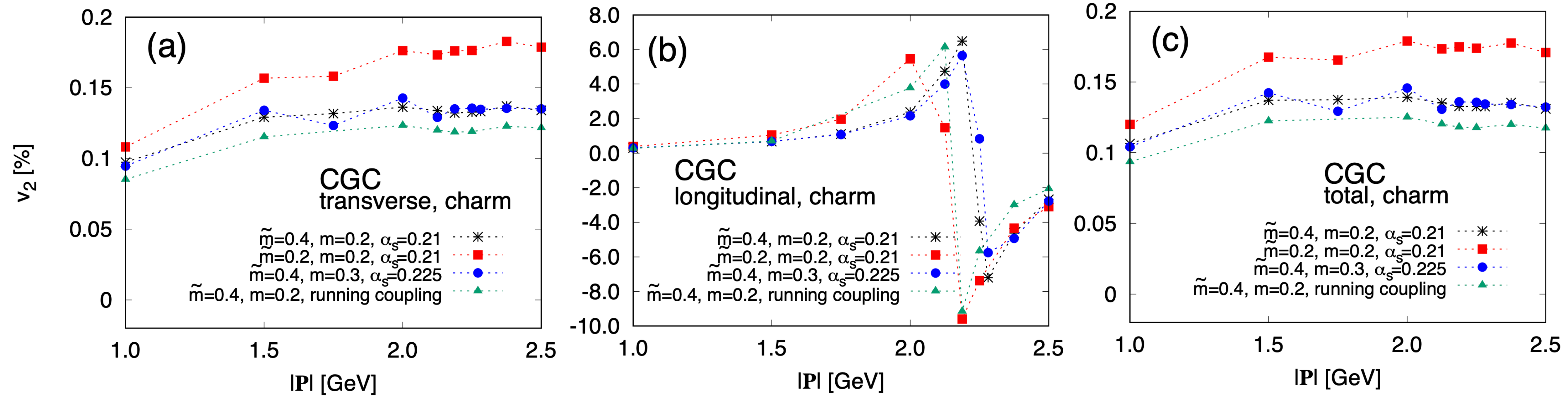


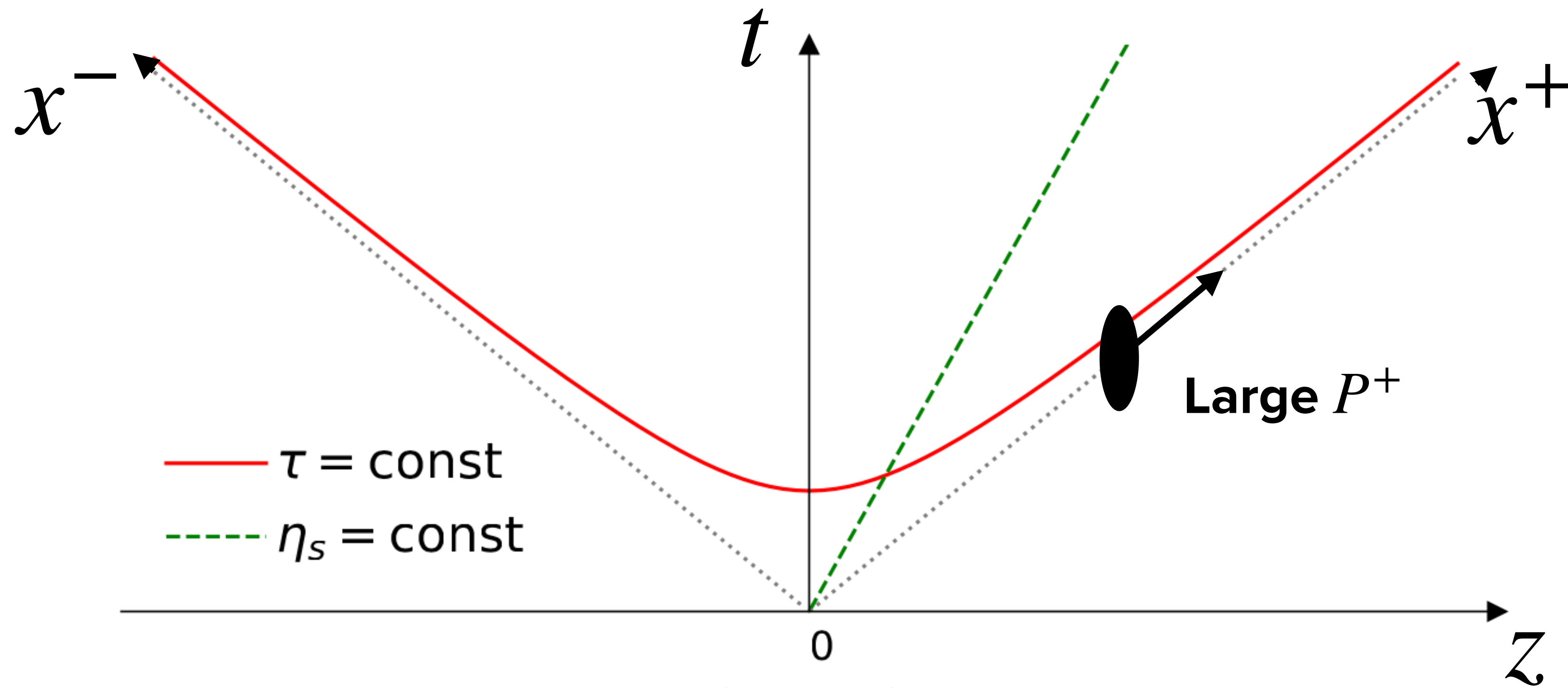
FIG. 16. Elliptic Fourier coefficients for the charm-dijet cross section for transversely (a) and longitudinally (b) polarized photons from the CGC for $|\Delta| = 0.1$ GeV, $Q^2 = 1$ GeV 2 . The v_2 of the total cross section is shown in (c). Results are integrated over $\theta(\Delta, \mathbf{P})$ and over $z \in [0.1, 0.9]$.

Summary

- Wilson lines are the building blocks of the Color Glass Condensate
- They enter all calculations at small x , in particular HIC initial state and the following:
 - Coherent and incoherent vector meson production (including x and $|t|$ dependence) sensitive to average nuclear shape and fluctuations!
 - Dependence of cross sections on angle between photon or vector meson and electron plane in DVCS and diffractive VM production, respectively. Can make connection to GPDs
 - Diffractive dijet production carries information on Wigner distribution/GTMD
- Some requirements:
 - Separate coherent and incoherent diffraction (for all $|t|$)
 - Measure jets to low p_T to be sensitive to saturation effects
 - Measure angular dependencies down to the percent level

BACKUP

Color sources

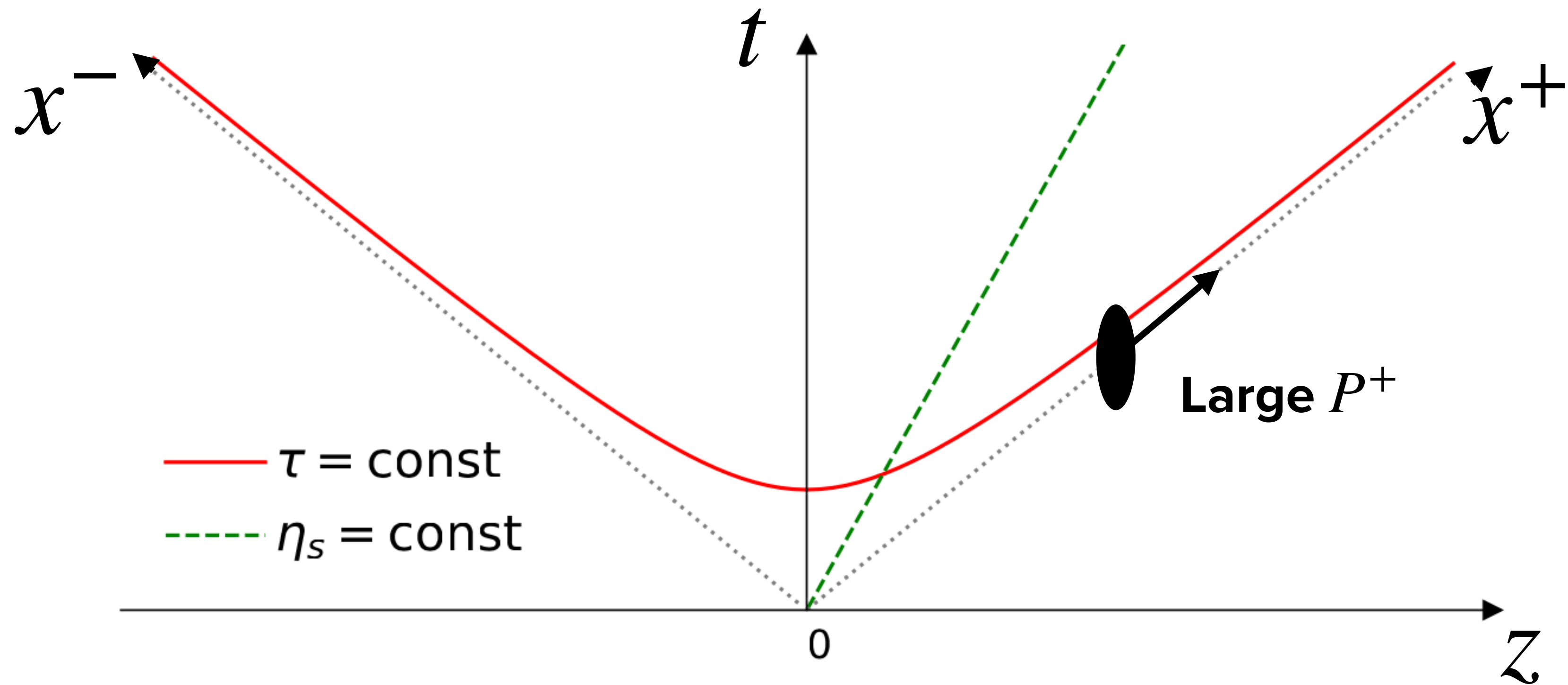


How localized are these sources? $\Delta z^- \sim \frac{1}{k^+} = \frac{1}{xP^+}$

What is the resolution scale of the probe? $\frac{1}{x_0 P^+} > \frac{1}{x P^+}$ for $x > x_0$

→ Color sources look fully localized to the probe in z^-

Color sources



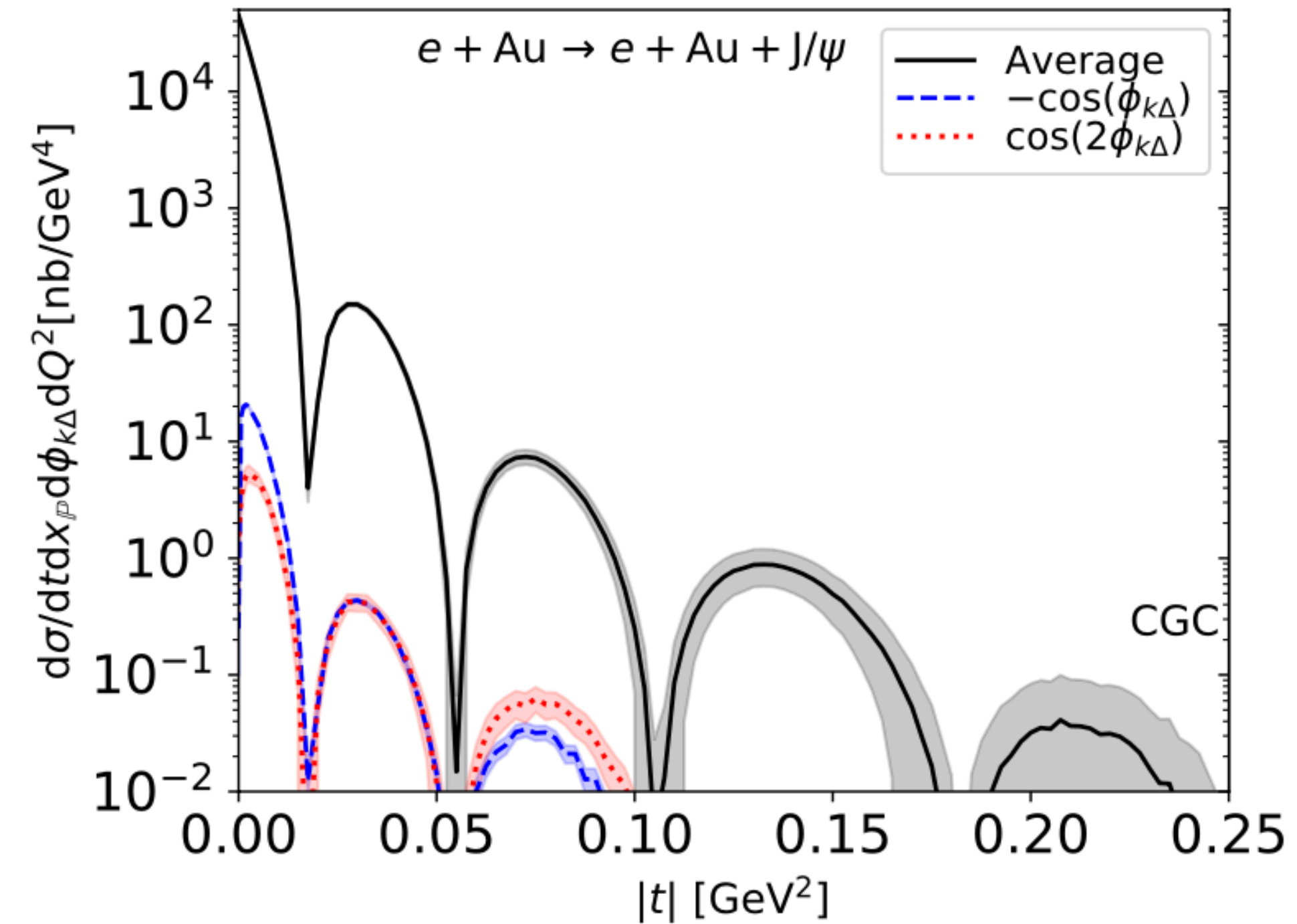
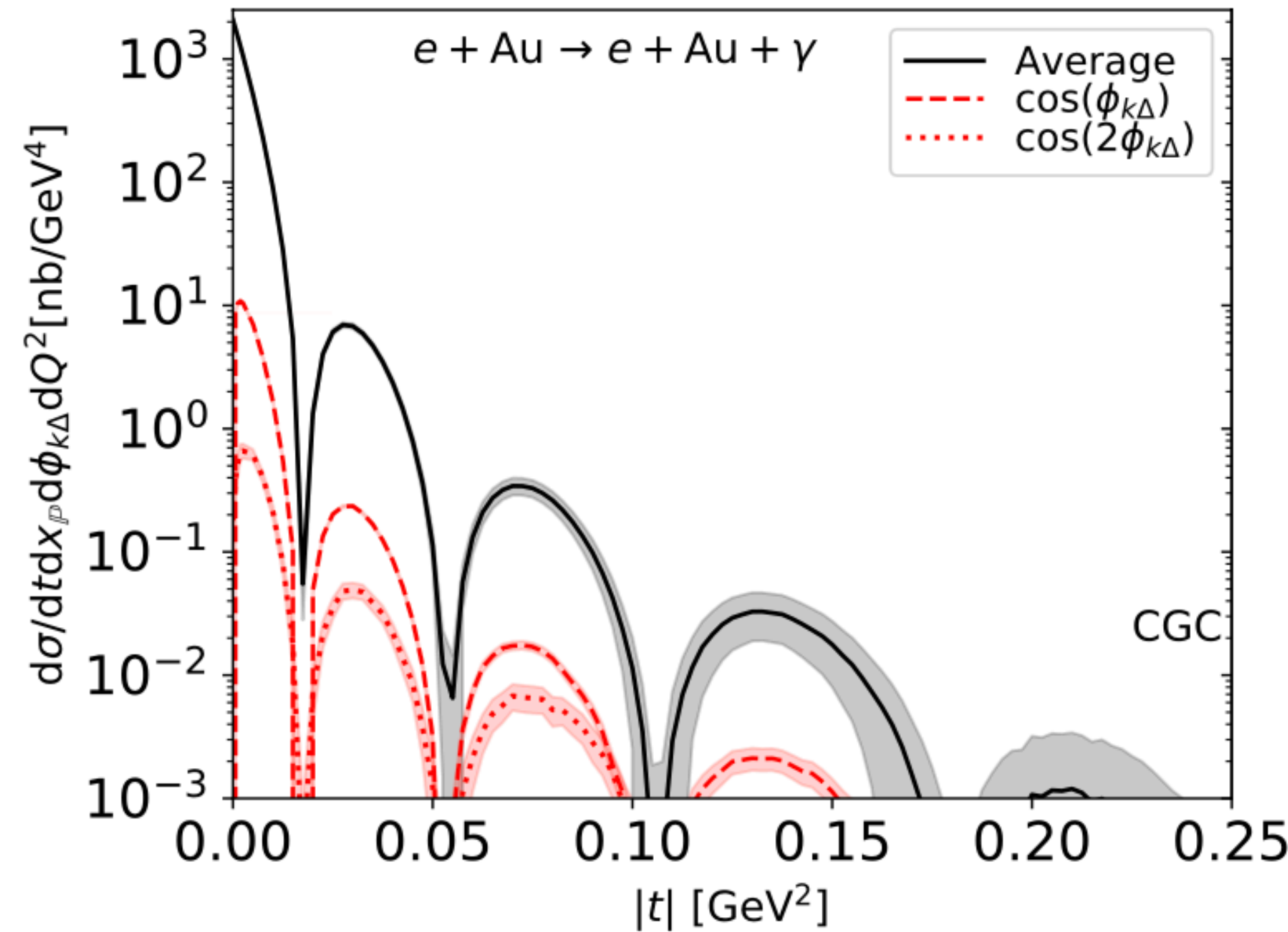
How fast do they evolve? $\Delta z^+ \sim \frac{1}{k^-} = \frac{2k^+}{k_T^2} = \frac{2xP^+}{k_T^2}$ (because $a_\mu b^\mu = a^+b^- + a^-b^+ - \vec{a}_T \cdot \vec{b}_T$)

What is the time scale of the probe? $\tau \approx \frac{2x_0 P^+}{k_T^2} < \frac{2x P^+}{k_T^2}$

→ Color sources look static to the probe in light cone time z^+

Predictions for e-Au at the future EIC

DVCS and exclusive J/ψ : Spectra and azimuthal modulations

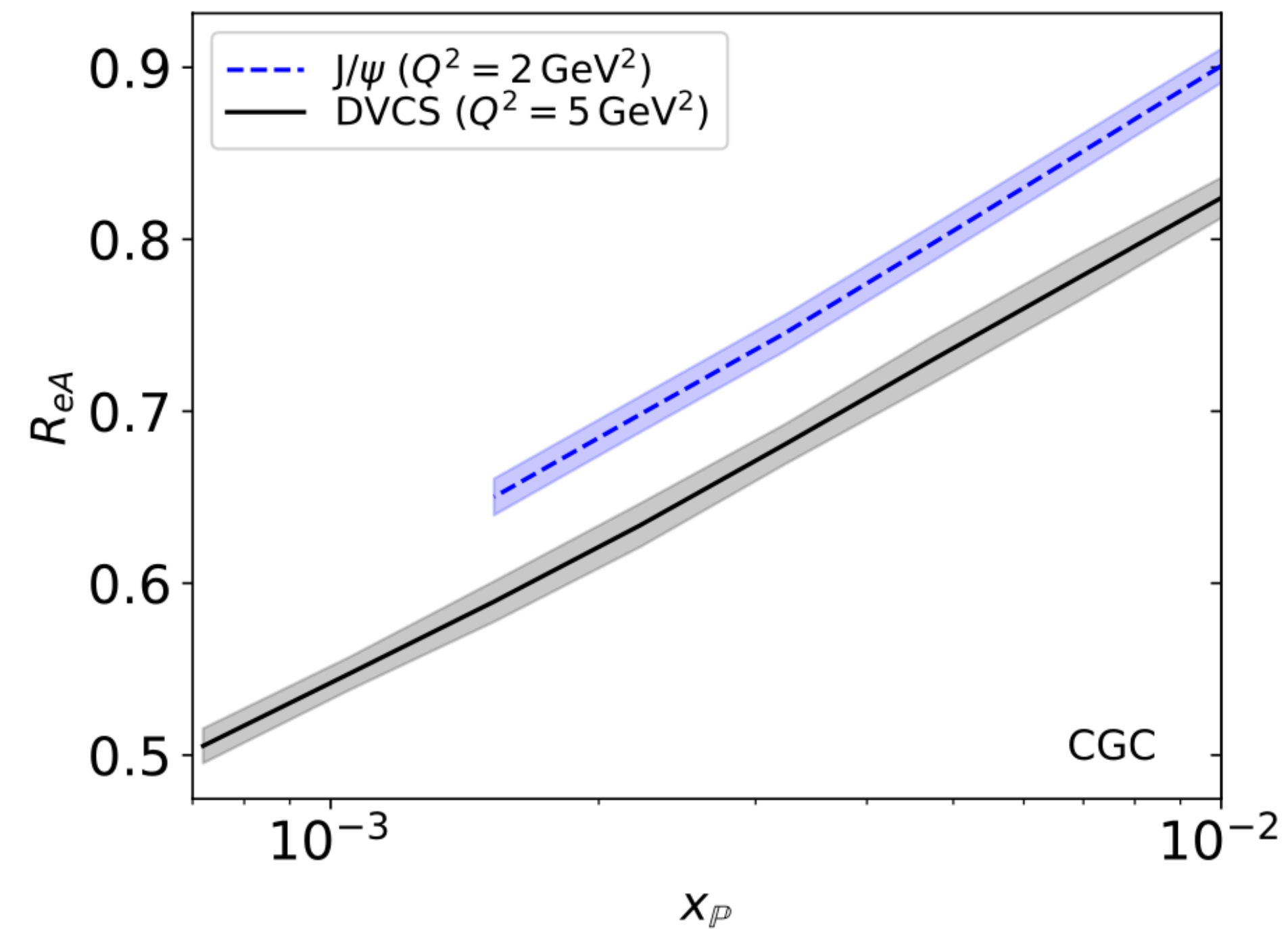


Characteristic dips in spectra due to Woods-Saxon nuclear profile

Azimuthal modulations v_n a few percent for DVCS, and less than 1% for J/ψ

Predictions for e-Au at the future EIC

Nuclear suppressions factor for DVCS and exclusive J/ψ



$$R_{eA} = \frac{d\sigma^{e+A \rightarrow e+A+V}/dt dQ^2 dx_{\mathbb{P}}}{A^2 d\sigma^{e+p \rightarrow e+p+V}/dt dQ^2 dx_{\mathbb{P}}} \Big|_{t=0}$$

Expect $R_{eA} = 1$ in the dilute limit.

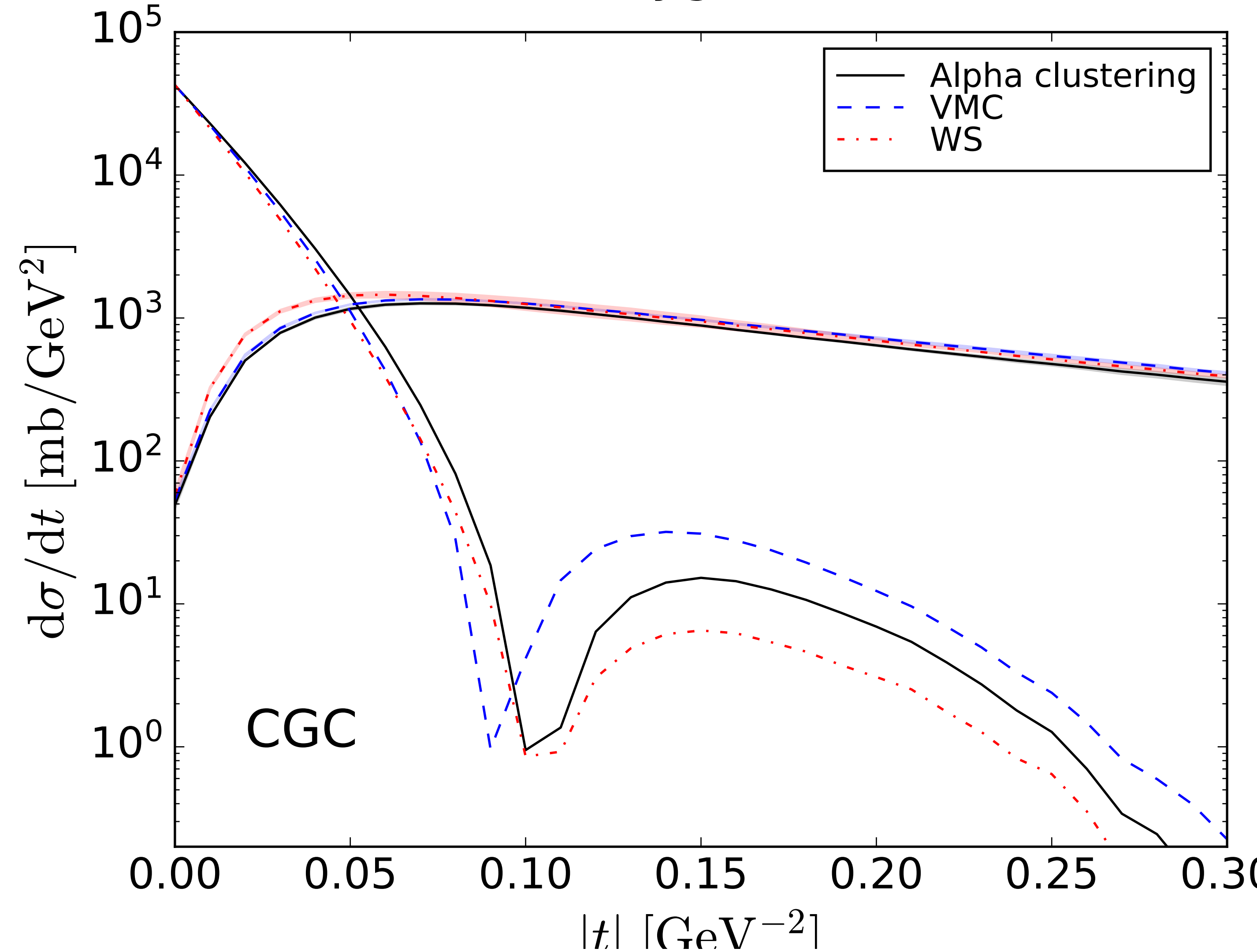
Mäntysaari, Venugopalan. [1712.02508](#)

Significant suppression that evolves with energy/ $x_{\mathbb{P}}$

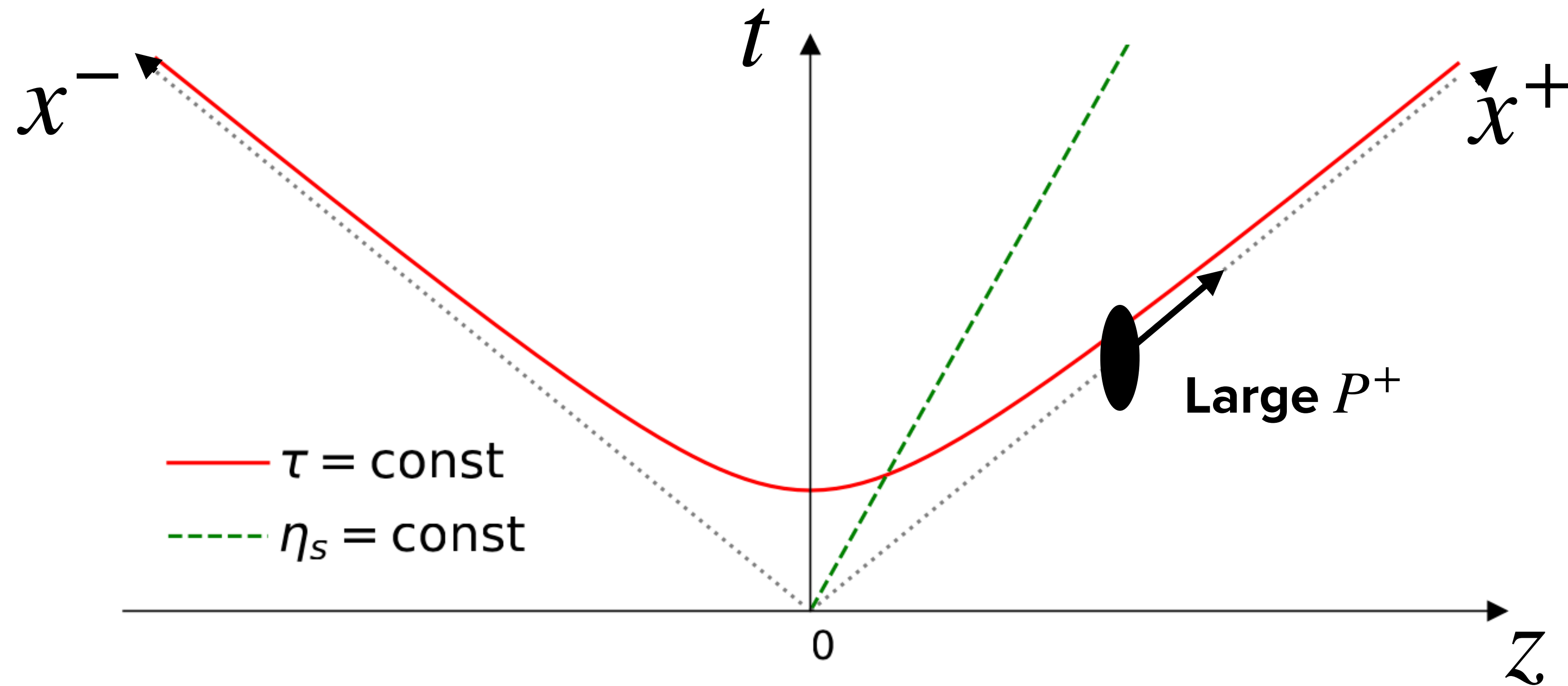
Larger suppression for DVCS due to larger dipole contributions.

e+O: Oxygen wave function dependence

oxygen



Light cone



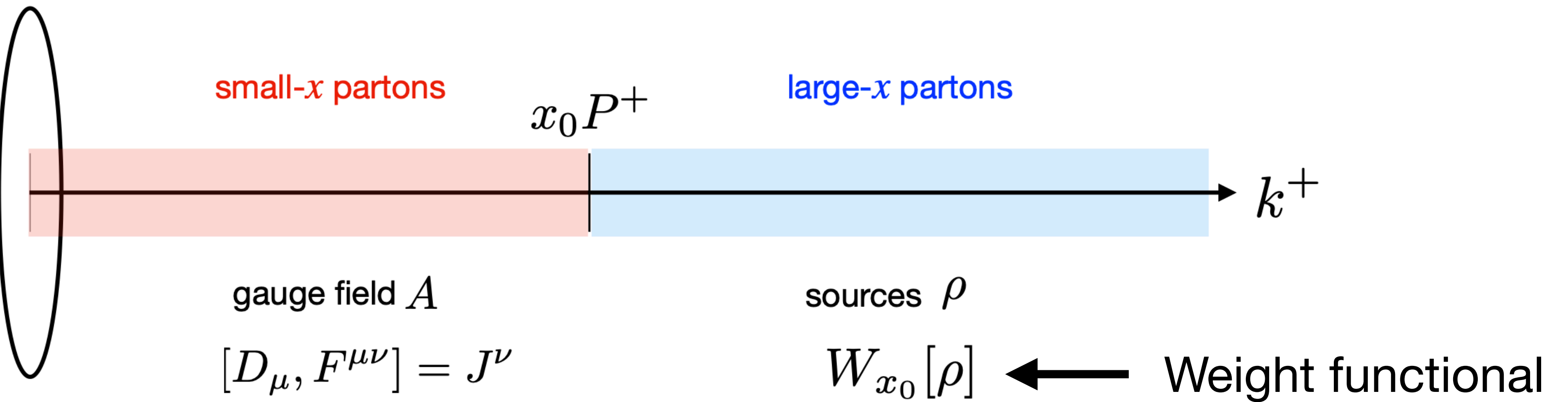
Light cone coordinates $v^\pm = (v^0 \pm v^3)/\sqrt{2}$

In the future light cone define $x^+ = \frac{\tau}{\sqrt{2}} e^{+\eta}$, and $x^- = \frac{\tau}{\sqrt{2}} e^{-\eta}$

or inverted $\tau = \sqrt{2x^+x^-}$, and $\eta = \frac{1}{2} \ln \left(\frac{x^+}{x^-} \right)$

Weight functional

<https://arxiv.org/pdf/hep-ph/0406169.pdf>



What is the weight functional?

Need to model. E.g. the McLerran-Venugopalan model:

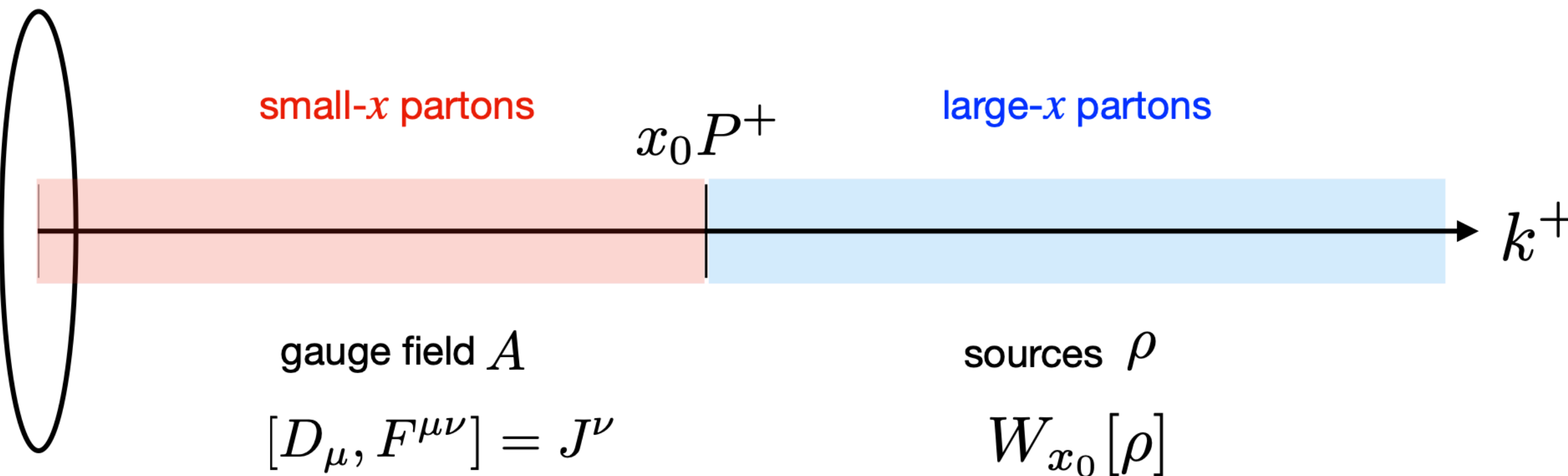
Assume a large nucleus, invoke central limit theorem. All correlations of ρ^a are Gaussian

$$W_{x_0}[\rho] = \mathcal{N} \exp \left(-\frac{1}{2} \int dx^- d^2 x_T \frac{\rho^a(x^-, x_T) \rho^a(x^-, x_T)}{\lambda_{x_0}(x^-)} \right)$$

where $\lambda_{x_0}(x^-)$ is related to the transverse color charge density distribution of the nucleus

Weight functional

<https://arxiv.org/pdf/hep-ph/0406169.pdf>



...where $\lambda_{x_0}(x^-)$ is related to the transverse color charge density distribution of the nucleus

$$\mu^2 = \int dx^- \lambda_{x_0}(x^-) = \frac{(g^2 C_F)(AN_c)}{\pi R_A^2} \frac{1}{N_c^2 - 1} = \frac{g^2 A}{2\pi R_A^2} \sim A^{1/3}$$

That color charge density is related to Q_s , the saturation scale.

normalized per color
degree of freedom